



Article

Forest Habitat Fragmentation in Mountain Protected Areas Using Historical Corona KH-9 and Sentinel-2 Satellite Imagery

Bogdan Olariu ^{1,*}, Marina Virghileanu ^{1,2}, Bogdan-Andrei Mihai ¹, Ionuț Săvulescu ¹, Liviu Toma ³ and Maria-Gianina Săvulescu ⁴

¹ Faculty of Geography, University of Bucharest, 010041 Bucharest, Romania;

marina.virghileanu@geo.unibuc.ro (M.V.); bogdan.mihai@unibuc.ro (B.-A.M.); savulescu@geo.unibuc.ro (I.S.)

² Romanian Young Academy, University of Bucharest, 050663 Bucharest, Romania

³ GISBox SRL, Bd. Timișoara 8A, 061344 Bucharest, Romania; liviu.toma@gisbox.ro

⁴ Simion Mehedinți Doctoral School, Faculty of Geography, University of Bucharest, 010041 Bucharest, Romania; maria.vladeanu@s.unibuc.ro

* Correspondence: bogdan.olariu@drd.unibuc.ro; Tel.: +40-744697938

Abstract: Forest habitat fragmentation is one of the global environmental issues of concern as a result of forest management practices and socioeconomic drivers. In this context, a constant evaluation of natural habitat conditions still remains a challenge in order to achieve a general image of the environmental state of a protected area for proper sustainable management. The purpose of our study was to evaluate the evolution of forest habitat in the last 40 years, focusing on Bucegi Natural Park, one of the most frequented protected areas in Romania, as relevant for highly human-impacted areas. Our approach integrates a historical panchromatic Corona KH-9 image from 1977 and present-day Sentinel-2 multispectral data from 2020 in order to calculate a series of spatial metrics that reveal changes in the pattern of the forest habitat and illustrate forest habitat fragmentation density. Object-based oriented analysis with supervised maximum likelihood classification was employed for the production of forest cover fragmentation maps. Ten landscape metrics were adapted to the analysis context, from patch statistics to proximity index. The results show a general growth of the forest surface but also an increase in habitat fragmentation in areas where tourism was developed. Fragmentation indices explain that larger and compact patches feature natural park protected forests after the spruce–fir secondary canopies were grown during the last 4–5 decades. The number of patches decreased to half, and their average size is double that of before. The method can be of extensive use for environmental monitoring in protected areas management and for understanding the environmental history connected to present-day problems that are to be fixed under rising human pressure.

Keywords: forest; habitat fragmentation; landscape change; remote sensing; image classification



Citation: Olariu, B.; Virghileanu, M.; Mihai, B.-A.; Săvulescu, I.; Toma, L.; Săvulescu, M.-G. Forest Habitat Fragmentation in Mountain Protected Areas Using Historical Corona KH-9 and Sentinel-2 Satellite Imagery. *Remote Sens.* **2022**, *14*, 2593. <https://doi.org/10.3390/rs14112593>

Academic Editor: Michael Sprintsin

Received: 21 March 2022

Accepted: 23 May 2022

Published: 28 May 2022

Publisher's Note: MDPI stays neutral with regard to jurisdictional claims in published maps and institutional affiliations.



Copyright: © 2022 by the authors. Licensee MDPI, Basel, Switzerland. This article is an open access article distributed under the terms and conditions of the Creative Commons Attribution (CC BY) license (<https://creativecommons.org/licenses/by/4.0/>).

1. Introduction

Forest habitat fragmentation is one of the first features to be investigated and assessed in the context of forest landscape configuration analysis on different scales, together with its structure, function and change [1–3]. It represents the most visible dynamic aspect of forest stand evolution [4]—a basic element of forest landscape change patterns at stand level in space and time [5,6]—to be modelled using integrated techniques of remote sensing and geographic information systems [7] at different scales, from local to regional, e.g., Rogan and Miller [8] in California, Ghosh et al. [9] in Northern India, up to the national level such as Heilman et al. [10] in the United States, Wulder et al. [11] in Canada, Singh et al. [12] or Reddy et al. [13] in India, and even at global levels [14,15]. In the context of global change, the biodiversity issue approach and modelling [16,17] is a task mentioned and explained in the framework of international/national programmes on the conservation of biological diversity after Rio 1992 [2], followed by earth observation-focused programmes, such as the

EOSD (Earth Observation for Sustainable Development of Forests in Canada, 1999, see [18]) and the European Space Agency (ESA) diversity project [19].

The factors of forest habitat fragmentation are different [20]—natural (topography, snow and ice, insects, fires) and anthropogenic (deforestation for timber and for agriculture or settlement development) and imprint on forest stand patterns [21].

Remote sensing data are known as a type of objective data collection to be integrated into mapping and modelling approaches, from simple analyses at the local scale to multi-temporal complex image analysis of change detection with the integration of big data from archives [22,23].

The first remote sensing and satellite image analysis-based approaches focused on forest fragmentation analysis, mapping and modelling are known from the 1990s, with contributions that focused on the largest forested regions, such as Amazonia [24], as well as on developing urban regions [25,26], with both employing Landsat imagery archives. It was in the same decade that authors searched for the implementation of robust quantitative indicators of the phenomenon, such as spectral indices [27]; however, interest focused on landscape metrics derived on the basis of classification products from multispectral imagery [28,29], taking into account the stage of data processing algorithms, and facilities availability also increased.

Over the last two decades, the forest fragmentation issue remains of outstanding interest, in the context of advances in satellite image data processing, from the calibration-validation [30] of products to classification and post-classification operations [31,32], but mainly because geostatistical approaches and software tools allowed for the production of important amounts of new data from satellite imagery archives, such as Landsat ETM+ [33] and other sensors such as the Indian launched IRS [34,35] or ASTER radiometric instruments [36].

One of the key directions of forest fragmentation mapping and analysis is the use of landscape metrics in searching for the most representative parameters of forest stand features, as explained in detail by [32]. Different contributions explained the most relevant parameters in forest fragmentation quantification and mapping [37] in the famous Rondonia area, Amazonia, a representative example of the process of deforestation and stand fragmentation.

Most authors have produced, validated and interpreted quantitative data based on landscape metrics and derived parameters extracted mainly from medium-resolution imagery classification and other image post-processing techniques [38], e.g., in the Argentina Chaco [39] forest region with prediction modelling [40], Zhou et al. [41] under urban developments of big cities in China and Bryan-Brown et al. [42] in mangrove-covered regions.

Other contributors have tried to model and explain, over the same time period, the contributing factors (Ramachandra, Setturu and Chandran [39] in India, Hermosilla et al. [43] in Canada, Armenteras et al. [44] in Brazil) and to open the results to the evaluation of the current state of forest stands as an indicator of biodiversity evolution trends [45], including field data collection [46] in India, Lawley et al. [47] in Australia, together with ecosystem services [48] in Amazonia, Brazil.

For regional- and local-scale approaches, and mainly for historical analysis of forest stand fragmentation, different authors have integrated aerial imagery with satellite data (Harper et al. [49] in Madagascar and Tapia-Armijos, Homeier, Espinosa, Leuschner and de la Cruz [36] in Ecuador), but the very challenging issue is the use of automatic and semiautomatic approaches in forest stand data layer production, such as object-based image analysis of the Azores islands with IKONOS imagery [50], Hernando et al. [51] on GeoEye imagery of Spain and Taubert et al. [52] in different tropical forest areas.

An increasing potential in forested landscape change analysis is represented by the declassified data of former spy satellites [53,54] with photogrammetric sensors and panchromatic imagery such as CORONA KH, HEXAGON, etc., e.g., Rendenieks et al. [55] in the Baltic states and Munteanu et al. [56] in the Romanian Carpathians. Although these data archives are free, their preparation for analysis and mapping needs typical photogrammet-

ric processing for orthophoto production and spatial accuracy assessment in order to adapt them to recent date imagery [57–59]. This is one of the directions of our current approach in the context of forest fragmentation multirate modelling in a representative protected area in the Romanian Carpathians.

Forest fragmentation in protected areas is a typical research issue for searching for innovative methodologies for landscape pattern analysis and mapping [60] and is a challenge in searching for new instruments for the sustainable management of biodiversity [61]. There are few contributions in this field based on landscape metrics derived from Landsat data, such as Gounaridis et al. [62] in Greece or Sahana, Sajjad and Ahmed [46] in India, IRS and other medium-resolution imagery in India [63], using fractal modelling in Bhutan [64], while Cheţan et al. [65] produced landscape metrics of forested landscapes in NATURA 2000 sites from the Apuseni Mountains, Romanian Carpathians.

Remote sensing mapping of forest habitat fragmentation is not a recent subject in the literature. Most papers employed imagery from the same sensors, such as Landsat, and/or combinations of imagery with similar spatial and even spectral resolution. These approaches are focused on large areas where spectacular results can be obtained such as tropical and boreal forest landscapes. The scale of analysis, together with image resolution, is a key factor in this type of approach (Linke, Betts, Lavrige and Franklin, 2006, Gergel, 2006). There are few contributions integrating higher spatial resolution data from historical declassified imagery, and most of them are less focused on protected areas and more on large areas with intensively harvested forest timber, such as the Eastern Carpathians (Niţă et al., 2018, Munteanu et al., 2021). Recent Sentinel-2 MSI data available from ESA Copernicus open new potential directions in land cover mapping and can bring a similar high-resolution update to landscape analysis that is in synergy with historical imagery (Nistor et al., 2021).

Our aim was the integrated use of multirate remote sensing images for forest fragmentation pattern change analysis and mapping of a well-known protected area in the Romanian Carpathians—the Bucegi Natural Park. This task is related to forest landscape change during the last five decades, in which former timber harvesting areas closed after 1990 were replaced by new forest stands and combined with older forest stands partly restored after World War II.

The objectives we proposed are: (1) CORONA KH-9 employment in a semiautomatic formula as a source for historical forest and dwarf pine stands pattern data layer after accurate orthophoto production, (2) the integration of these data with Sentinel-2 MSI derived data from 2020 representing the current configuration of the forested landscape and (3) a statistical approach using fragmentation degree change during the reference period, starting from the adapted landscape metrics, and explanation of the effects of forest stand protective management on habitat fragmentation under the natural park regime of the study area.

The next section, Materials and Methods, presents the study area and data sources that were used in order to perform the analysis, along with their technical characteristics. In addition, we included a detailed explanation of how the Corona KH-9 image was processed since it is relatively new to geographical studies. Furthermore, we present the methods that we used for obtaining the two classifications and fragmentation data, which appear on our maps.

In the Results section, we present the maps that show the land cover (forest area) in and level of fragmentation of the Bucegi Natural Park, along with some explanations regarding the distribution of fragmentation values in some areas, considering why score values are low in some parts of the reservation and high in others.

In the Discussion section, we associate our results with other data and perform secondary analysis in order to obtain more data and cross-validation. First, we present a validation of the two classifications so that we ensure that all our data are relevant for further analysis. Afterwards, we analyse a series of landscape metrics for forest habitat fragmentation, which can be associated with the high values of fragmentation in some

areas. At the end of the section, we compare our fragmentation data with the protection-level maps from the natural area. This is to emphasise the importance of environmental degradation and evaluation.

In the Conclusion section, we draw on a few ideas about the usefulness of historical satellite images in comparison with newer ones, together with some facts regarding the evolution of the forest in the studied area and the utility of the analysis for institutions and further research.

2. Materials and Methods

2.1. Study Area

The Bucegi Mountains, together with the Upper Prahova Valley (Figures 1 and 2), represent the most popular mountain tourism area of the Romanian Carpathians and a starting point of tourism history in Romania [66]. At the same time, it is a problematic area in the context of the intensification of tourism-related activities, such as trekking or mountain biking, as well as skiing.



Figure 1. Bucegi Mountains—Coștila Peak (2490 m), with an 80 m high communication mast, making it the highest artificial point in Romania, on top of Abruptul Prahovean and part of the upstanding syncline eastern ridge (Photo: B. Olariu).

The Bucegi Mountains cover an area of 395 km² and feature great landscape variety related to geological and structural aspects, especially altitudinal development. The area has important geodiversity, with structural relief, lithological landforms, glacial and periglacial landscapes, and is composed of scenic landscapes that became an icon of Romanian mountain tourism from the first tourist guidebooks at the beginning of the 20th century.

The Bucegi Mountains land cover [67] is varied and complex and developed on clear altitudinal zones: the beech forest zone from 700 to 1200 m, including a transition zone of mixed forests between 1200 and 1450 m with beech, fir and spruce–fir stands; the spruce–fir forest zone between 1450 and 1800 m; the Subalpine zone between 1800 and 2200 m, where the dwarf pine (*Pinus mugo*) is the primary vegetation, is now limited to some patches on the main plateau area; and the alpine zone, higher than 2200–2250 m of meadows with rocky zones.

This complex landscape is the subject of a protected zone of the Bucegi Natural Park, a protected area from the IUCN Vth category, and covers about 327 km². Its foundation is related to the first protection efforts from 1930 [68], in the context of increasing interest in mountain tourism in the Bucegi-Prahova Valley region, but it was not until 2000 that real protection was offered, indicated by the first management plan for the park. The protected area covers the biggest part of the massif (Figure 1), from the edge of Sinaia and

Bușteni towns and the eastern slopes to the western and northern ones, with nine reserves with special regimes. Three of them protect alpine and subalpine landscapes (“Abruptul prahovean” reserve is the largest—Figure 1) on the structural escarpments, while others protect caves and rock outcrops with fossils occurrences.

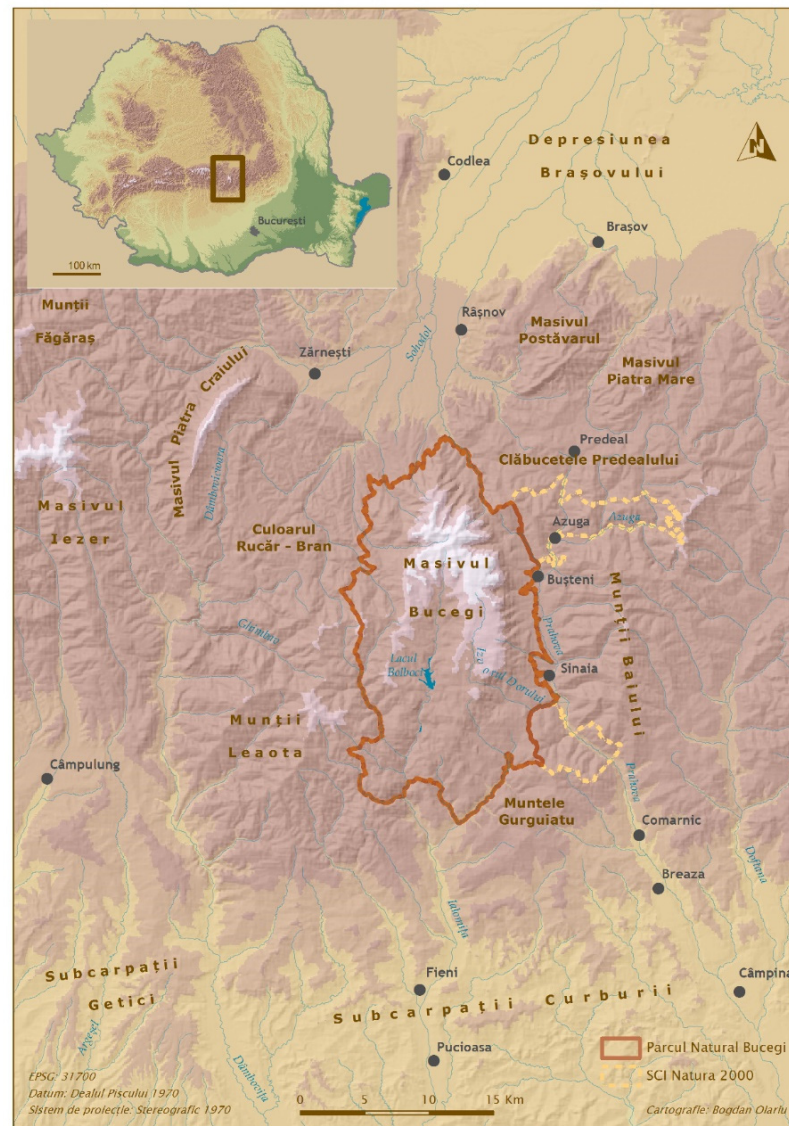


Figure 2. Study area.

This protection regime allows tourist activities and even grazing in selected areas and forbids these activities within some perimeters where landscape elements of scientific value are dominant. Landscape evolution of the latest century shows a double polarisation of human impact on the extreme zones, the Bucegi Plateau and the Prahova Valley, between Sinaia and Bușteni towns and tourist resorts (750–900 m).

The current configuration of the Bucegi Natural Park’s protected perimeter, as stated in 2016 [69], allows the continuity of tourist traffic along the traditional paths, together with grazing on selected neighbouring slopes, and does not create conditions for environmental recovery. Soil erosion is now a real problem that has intensified during the last three decades, with an accelerated rhythm during the last decade.

The study area’s complex land cover and forest cover mapping is still a challenging subject. Spatial data infrastructure for protected area management is limited, rather general and out of date. This is the reason for the search for new tools to be actively integrated with

other layers in the search for sustainable management. Remote sensing data integration can help, but only if it is possible to extract current situation spatial features in close relationship with the past configuration of forest canopies. This needs adaptation to a detailed spatial scale and temporal coverage to explain the changing patterns. This is the reason the methodology needs to follow two totally different directions: a photogrammetric workflow, together with image classification, followed by a quantitative part and interpretation.

2.2. Methodology

Our analysis focuses on the integration of two optical remotely sensed images captured at different temporal moments: a declassified KH-9 Hexagon satellite photograph from 1977 and a multispectral Sentinel-2 MSI satellite image from 2020 (Table 1) (Figure 3).

Table 1. Remote sensing datasets used in the analysis.

Dataset	Acquired Date	Spatial Resolution	Sensor	Description	Source
KH-9 Hexagon	8 October 1977	9 m	Frame camera	1-band scanned grayscale image, 8 bit	USGS digital archives ¹
Sentinel-2 MSI	31 August 2020	10 and 20 m	Multispectral	13-band scene covering the visible and infrared spectra, 16 bit	ESA Copernicus SciHub ²

¹ <https://earthexplorer.usgs.gov/> (accessed on 25 August 2019); ² <https://scihub.copernicus.eu/> (accessed on 15 May 2021).

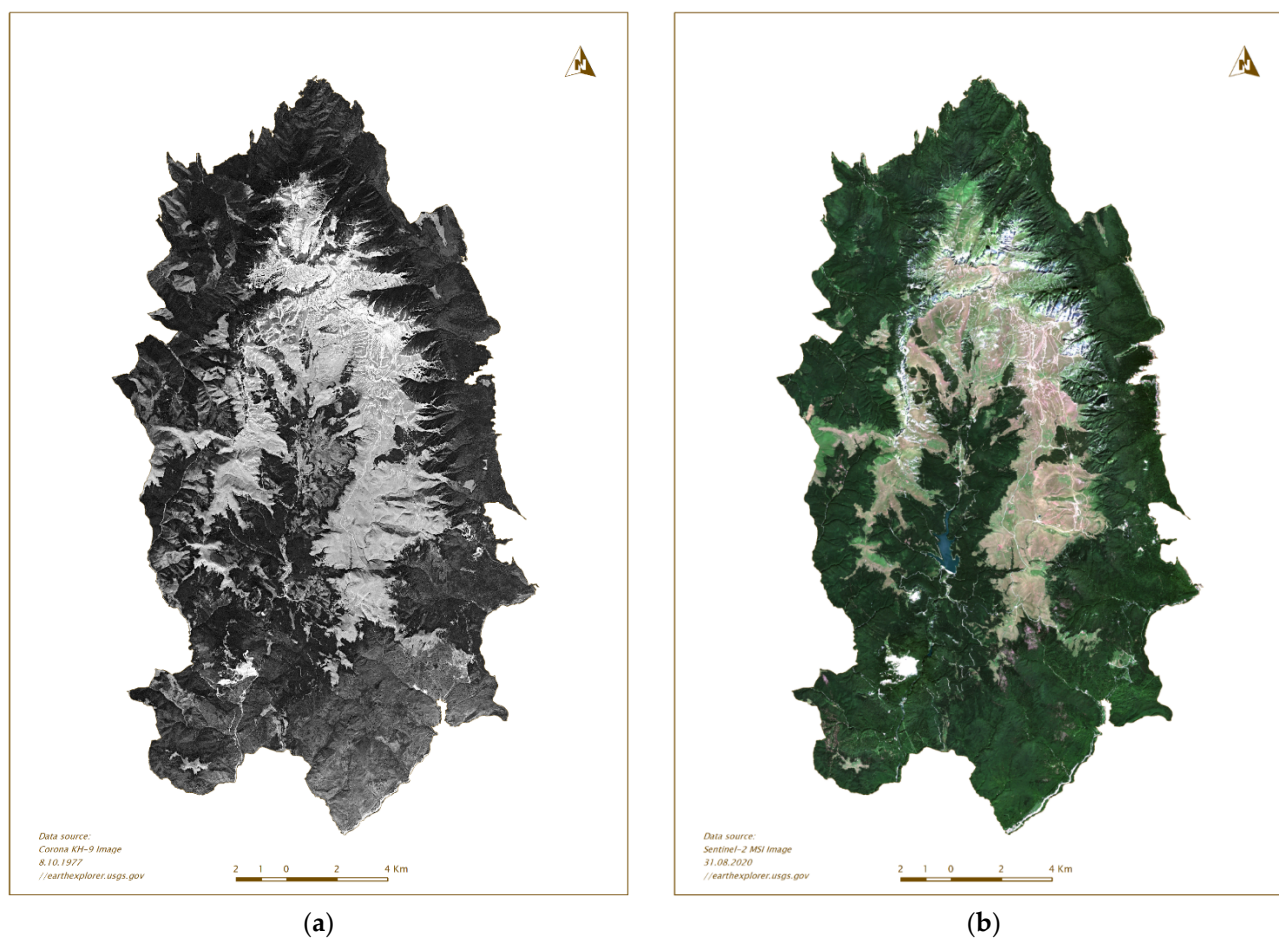


Figure 3. Bucegi Natural Park diachronic satellite imagery data coverages: (a) panchromatic image Corona KH-9 from 1977; (b) multispectral image Sentinel-2 MSI from 2020. Data sources: (a) <https://earthexplorer.usgs.gov/> (accessed on 15 September 2018); (b) <https://scihub.copernicus.eu/> (accessed on 25 August 2020).

The KH-9 Hexagon images, collected by the United States over the USSR and China between 1971 and 1986 as a continuity of the Corona mission, were declassified starting from 2000, being available free of charge through the USGS (United States Geological Survey) data platform [70]. Being captured by a frame mapping camera and later scanned in order to include them in digital archives, the KH-9 images are affected by radiometric and geometric errors and discontinuities [71,72], requiring calibration and correction processing steps before data extraction. However, the high spatial resolution of about 9.0 m offers good opportunities for detailed mapping and for data integration with new satellite products.

The Sentinel-2 (S2) MSI images are acquired from the ESA Copernicus programme, starting in 2015 with a revisiting period of 5 days. Collected by a multispectral sensor, the S2 scenes contain 13 spectral bands covering the visible, red-edge and infrared spectral domains at a spatial resolution of 10, 20 and 60 m, making them suitable for various applications and automatic processing [73–75]. The freely available datasets are delivered through the ESA Copernicus SciHub at two levels of processing, including the Level-2A calibrated data in terms of surface reflectance used within this study.

Our approach focused on three main processing stages, as presented in Figure 4. The first step corresponds to the photogrammetric processing of the KH-9 Hexagon image.

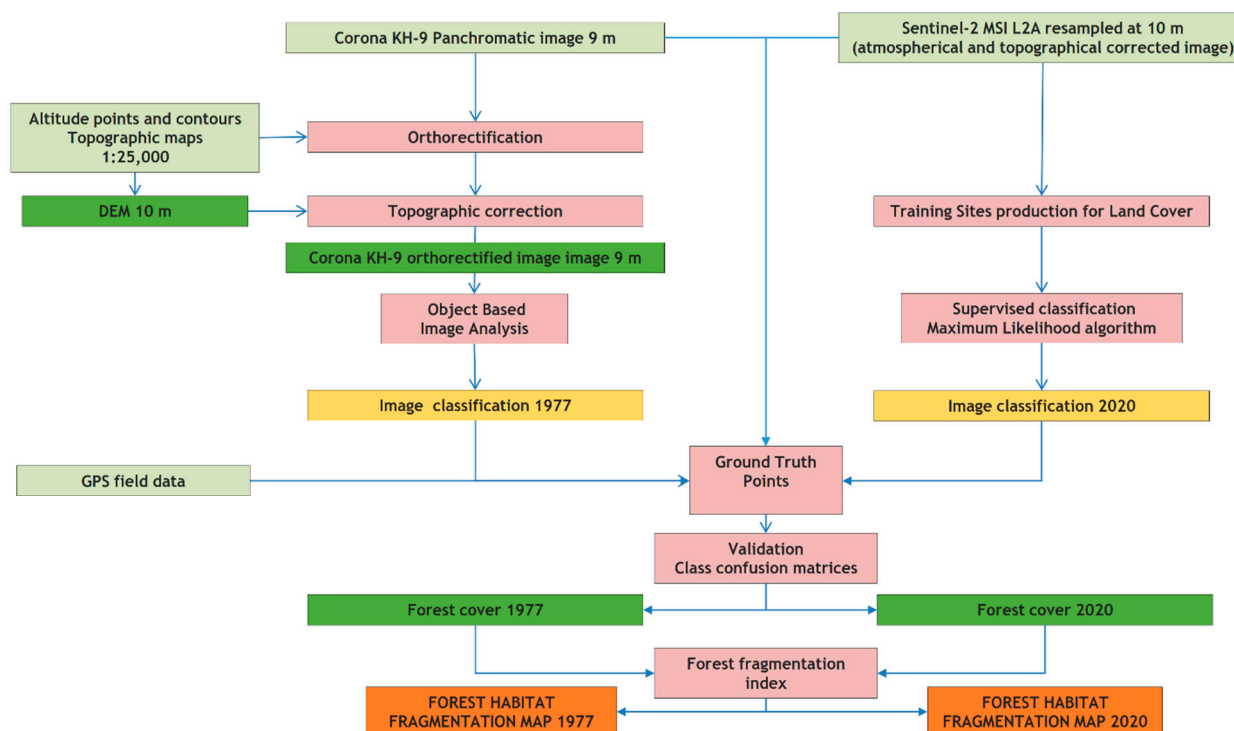


Figure 4. Workflow of the analysis.

HEXAGON KH-9 (or Keyhole-9) panchromatic image processing is a challenging task of our approach and an essential issue because of the need for high-accuracy historical data for forest stand classification and mapping. The primary image from the DECLASS-1 collection, available in the USGS Earth Explorer archives [76], is a scanned copy of the original film frames with geographical references of the four corners of each of them.

For the study area, it was used as an accurate data subset, extracted from an orbital stereo (vertical) coverage from the southern to the NE part of Romanian territory, consisting of six KH-9 cartographic frames [77], mission 1213 (dated 10 August 1977) and covering around 1/5 of the country surface.

The KH-9 data processing was accomplished based on a standard photogrammetric process, in which an aerial block triangulation based on bundle block adjustment with GCP (ground control points) support generated a precise camera model for the KH-9 frames.

Software solutions were based on a combination of tools from Socet Set v5.4.1 and Orima TE/GPS 9.0a, together with a complete Inpho/Trimble processing suite.

With the help of the basic data of the KH-9 cartographic (terrain) camera [77] and scanned digital image (focal length 305 mm, maximum 100 μm radial and 20 μm tangential distortions, image frame format 23 cm \times 46 cm, 7 μm resolution and an 8-bit depth), the photogrammetric process started with the building of the interior orientation of the image frame.

Project definition and initial relative orientation model building were possible only by providing the GPS/IMU (global positioning systems/inertial measurement unit) data for the referenced image frames. Initially, a local CRS (coordinate reference system) was associated with the frame, needing registration to a GPS-recognised coordinate reference system. The GPS positioning data, based on initial image metadata, were automatically approximated with respect to the new image's centre positioning on the local reference system, Stereo70. For the angular units, the kappa angle was deduced from the orbital satellite angle value, while the omega and phi angles remained zero.

For improvement of the geometric accuracy of the image model, a collection of well-distributed ground control points was used.

With the help of Socet Set v5.4.1 and Orima TE/GPS 9.0a, two complete processes were fulfilled based on analogue and digital interior orientation definitions. No major differences could be taken into account, as both independent camera-calibrated models, created by aerial triangulation, with GCP support (a total of 41 GCP as the control and 5 GCP as the check dataset), fit to a general sigma zero reference value of 9 μm (+/− 10%), with a GCP RMSxy (root mean square error on xy axes) of 4.6 m and an RMSz of 3 m for the control points, and an RMSxy of 5 m and RMSz of 7 m for the GCP set used as the check dataset (maximum deviation 6 m on the X-axis, 8 m on the Y-axis and 10 m on the Z-axis). The final bundle block adjustment, based on system autocalibration, had only one constant parameter—the camera focal length. The PPA (camera-calibrated principal point axis) and the radial distortions were the main variables, followed in order by other additional parameters related to affinity and nonorthogonality, nonflatness, as well as other uncompensated deformations of the frame model.

The final accuracy control of the block bundle adjustment (with autocalibration) was completed in a stereo environment in which a good model accuracy was obtained, with some small parallax on the area where the GCP influence was lower. This led to the conclusion that almost similar spatial accuracies can be obtained after an increase in the GCP number from 1 point/1, 250 km² to 1 point/500 km², with a final medium distance between the GCP positioning of around 20 km length (an appropriate value for KH-9 image frame autocalibration, by aerial triangulation bundle adjustment and with GCP support).

For quality purposes, with an additional number of 65 GCP (from the National Geodetic Network), an alternative data processing with complementary software such as Trimble Match-AT/aerial triangulation (digital interior orientation case), with a calibration based on 44 additional parameters, helped the production of an improved bundle block adjustment, with a sigma zero/nought of 6.7 microns and lower RMS values (less than a half of the GSD) for the XY and also the Z-axis (maximum deviation of GCP residuals less than 3 m on XY and Z).

The main differences between Socet SET/Orima and Trimble Match-AT consisted of better APM (automatic point matching) strategies (LSM (least squares matching) combined on different levels with FBM/ABM strategies) and better automation and precision of the APM process, with no manual tie points required for MATCH-AT APM process completeness. The RMSxy of automatic points in the photo (more than 4000) was less than 4 μm , with maximum residuals of 19 μm for all six image frames. At the same time, the autocalibration of the KH-9 cartographic camera model was slightly better, defined by the latest implemented processing algorithm of Trimble Match-AT.

Derived from a scanned frame resolution of 7 μm and in the context of a flight altitude of approximately 165 km, the KH-9 image frame block has a final resolution of 3.8 m.

The obtained accuracy of all results fell within the recommended limits indicated in the literature [78].

Digital elevation data coverage from the aerial triangulated data fitted to the upper limits of Level 1 acceptance [79], with 12.43 m RMSz for Socet Set processing and 14.5 m RMSz for the Trimble Match-T DSM (digital surface model). Overall, even though the resulting DTMs could be properly used for the image rectification process, due to some local DTM generation discrepancies caused by a lack of image contrast, the final orthoimage production used an enhanced independent model derived from 1:25,000 topographic maps, with an overall RMSz accuracy of 3 m. As a general aspect, if no stereo DTM enhancement can be fulfilled, especially for very large area coverage, the usage of an accurate DTM independent model is preferred.

After resampling the new data layer with the help of the Trimble OrthoMaster software tool, together with Trimble Ortho Vista and Trimble Seam Editor, the Orthoimage mosaic derived from the KH-9 imagery (Match-AT digital case processing) fitted to Level 1 acceptance criteria [79], with an RMSxy value of 4.61 m (1.2 × GSD, ground sampling distance) and a maximum 8.90 m local deviation. A map of errors on selected GCPs confirmed good results for the Bucegi Mountains area, our study area, for the highest and lowest altitudes after Trimble Match-AT processing (4–5 on the high plateau, lower than 4 to the foot of the mountains). It is an encouraging factor for basic image production for classification purposes.

The resolution of this historical data coverage (with a GSD of 3.8 m calculated after block triangulation) confirms that the data can be used for object-oriented approaches, although the spectral resolution is limited to a typical film frame-derived digital panchromatic image. Despite the difficulties in Corona KH imagery photogrammetric processing, their quality in forest studies and especially in forest disturbances modelling (deforestation) is recognised in detailed scale approaches in the Romanian Carpathians [80].

The second stage is represented by semiautomatic classification of the calibrated satellite imagery for forest cover data production. Different approaches were applied to each dataset, as the input images have distinctive features.

The orthorectified KH-9 Hexagon image was the subject of object-oriented image analysis (OBIA) following two processes [81]: (1) image segmentation for object delineation and (2) classification of the objects into two classes (forested area and non-forested area) using the support vector machine algorithm. Thus, training samples were provided for the algorithm in order to perform the classification, setting a polynomial Kernel type with a degree of 2 and a probability of 120%. The threshold was set to 5. Expert knowledge from terrain observation and visual image interpretation, including historical analogue aerial photos from the early 1970s, had a key role in the image segmentation process. Finding the best-scale parameter for object detection is based on the combined application of grey level and textural criteria in close relationship with the topographic position of vegetation patches and canopy elements, from forest stands to dwarf pine subalpine stands.

The KH-9 image classification was performed as an iterative process, focusing on finding the best options for object delineation and classification, as the single grayscale band and the radiometric distortions of the image cause multiple errors, especially in mountainous areas with rough surfaces and various vegetation layers, as was the case in our study area. Therefore, for the Bucegi Natural Reserve area, the OBIA returned better results when the image was split by altitude and vegetation types. In this context, the classification was run twice, applying alternative masks on the image, below and under 1350 m.a.s.l., considering the transition line between beech and spruce forest zones. The resulting datasets were then merged and filtered using the terrain topography in order to eliminate the errors imposed by slope degrees under 45° and altitudes under 2100 m.a.s.l. Finally, a classification confusion matrix approach [82] was applied in order to evaluate the accuracy of the forest cover dataset by using a total number of 200 ground control points extracted from the initial image by visual interpretation and field observation during different seasons (2013–2021).

The forest cover feature extraction from the Sentinel-2 image followed a thematic supervised classification approach, as the high spectral resolution helped this process. The training dataset referring to various land cover features (such as deciduous, coniferous, pastures, etc.) (Table 2) was created based on the input image, as well as on orthophotos and field data. The maximum likelihood classification algorithm was preferred because of its best performance in situations when the land cover classes are more homogenous [67,83]. The classification algorithm calculates the probability of associating with a class of every pixel value, which, in the end, is associated with the highest value of probability. The forest cover features extracted from the classification results were generalised in order to remove the isolated polygons with an area smaller than 500 m². This perimeter was chosen for further relevant analysis of habitat fragmentation. The validation was performed with the help of another confusion matrix, based on a total number of 200 random ground control points. Their value was extracted separately from the satellite image. The validation was performed using only the forested areas extracted from the satellite image of Sentinel-2, thus making it comparable with the forest cover from Corona KH-9. The ground truth points were marked as the presence/absence of forest cover in each of the images.

Table 2. Land cover classes and number of samples used for supervised classification on Sentinel-2 MSI image.

No.	Land Cover Class	Number of Samples	Areas Used for Validation
1	Coniferous forest	24	✓
2	Deciduous forest	49	✓
3	Dwarf pine (<i>Pinus mugo</i>)	26	✓
4	Mixed forest	10	✓
5	Pasture	52	X
6	Cliff area	37	X
7	Water	29	X
8	Built-up area	51	X

The third stage of the analysis focused on forest habitat fragmentation and analysis. This was adapted to the specific features of the forest stand fragmentation mapping. In this regard, the forest fragmentation index was calculated for each reference time on a 500 m × 500 m spatial grid by the following formula:

$$\text{Forest habitat fragmentation index} = \frac{\text{lenght of forest selvage (km)}}{\text{forest surface (sq. km)}} \times 100$$

Different spatial metrics [84] were also applied for each dataset in order to quantify and compare the forest cover structure and pattern. These are selected and interpreted according to the relevance of the results in connection with the maps.

3. Results

The maps of forest cover in the Bucegi Natural Park are the results of forested area classifications as explained. Figure 5 corresponds to the processing results of the KH-9 image from October 1977 and of the Sentinel 2-MSI image from August 2020.

The older forest cover map (1977) (Figure 5a) shows the topographic influence on the forest zones of the massif, where steep slopes of the escarpments limit the timberline and represent a natural factor of forest habitat fragmentation. It is easy to observe a fragmented landscape featuring all the most accessible valleys, where forest roads and cable timber transport lines, together with narrow-gauge railroads, created many logging points during the first half of the 20th century. The map depicts a better situation after the systematic restoration of some selected stands between the 1950s and 1970s and the limiting of timber harvesting and local economic activities in the Upper Ialomița basin.

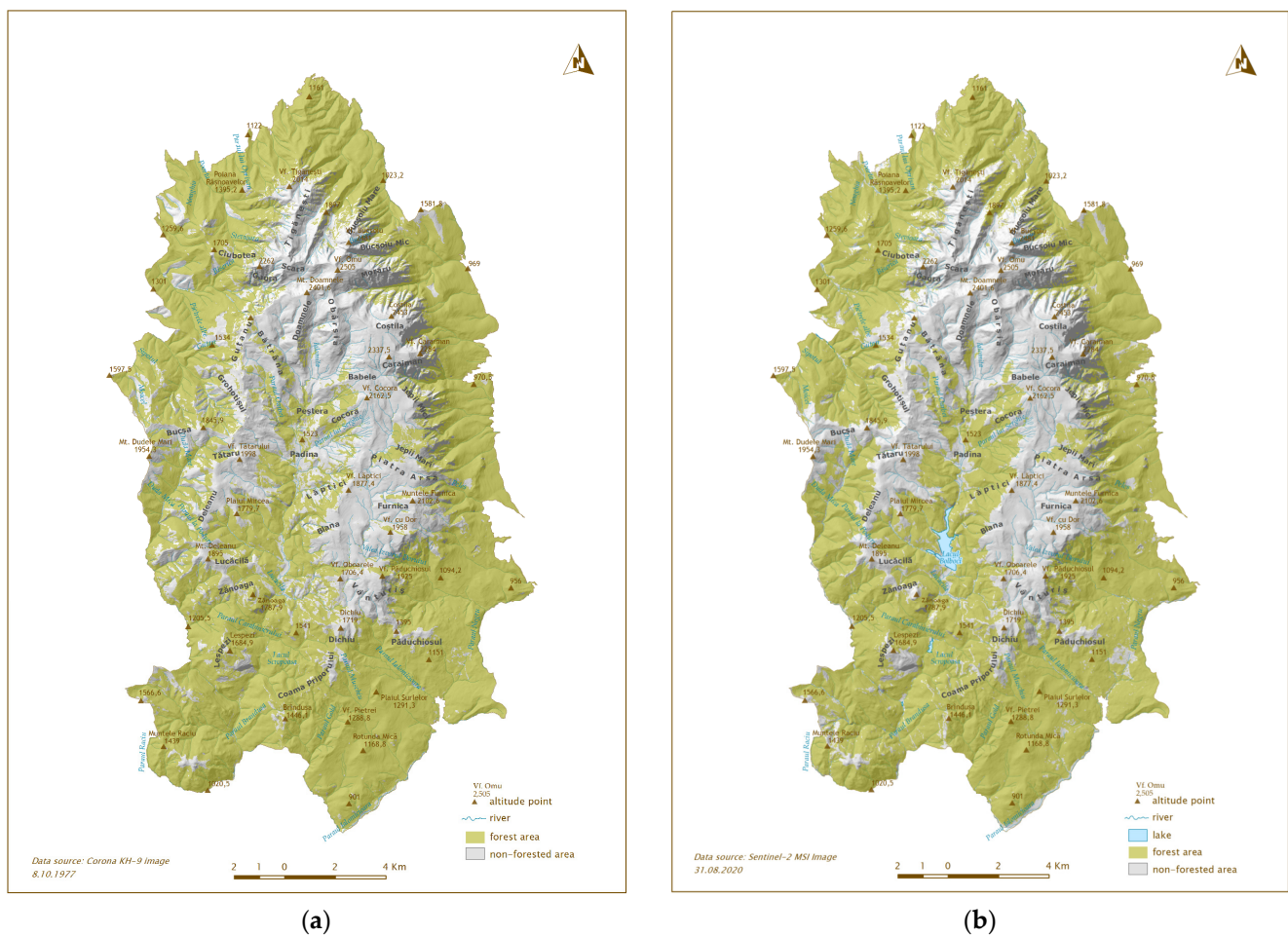


Figure 5. Bucegi Natural Park, forest habitat maps for (a) 1977 and (b) 2020.

The recent forest cover maps of the Bucegi Natural Park (2020) (Figure 5b) are an image of a period of forest configuration after two decades of natural park management. There is a slight trend in forest stand recovery on some slopes. Another aspect is the decrease in forest fragments in the Upper Ialomița Valley and in other valleys known as timber harvesting areas in the previous decades. Dwarf pine patches on the subalpine zone of the massif are limited to compact areas on the plateau around the Piatra Arsă zone, an effect of the intensification of erosion processes.

Figure 6 reveals the habitat forest fragmentation maps of the Bucegi Natural Park area for the two periods: 1977 and 2020. The fragmentation intensity is described by five classes, with values ranging between zero, corresponding to near intact forest habitats, and 144, meaning severe forest habitat reduction. The higher the value of the fragmentation index means that the forest habitat has a rising tendency to be replaced by other habitats, such as pasture or eroded land, an effect of grazing/overgrazing (plateau, southern part) and tourist traffic and developments (central and northern Bucegi plateau).

The map of the initial state (1977) (Figure 6a) reveals a combination of patches with high degrees of fragmentation on the Upper Ialomița Valley above and around the main junction area and some of its tributaries downstream the timberline areas. It is a situation created by continued logging combined with systematic forest stand recovery that started after the 1950s.

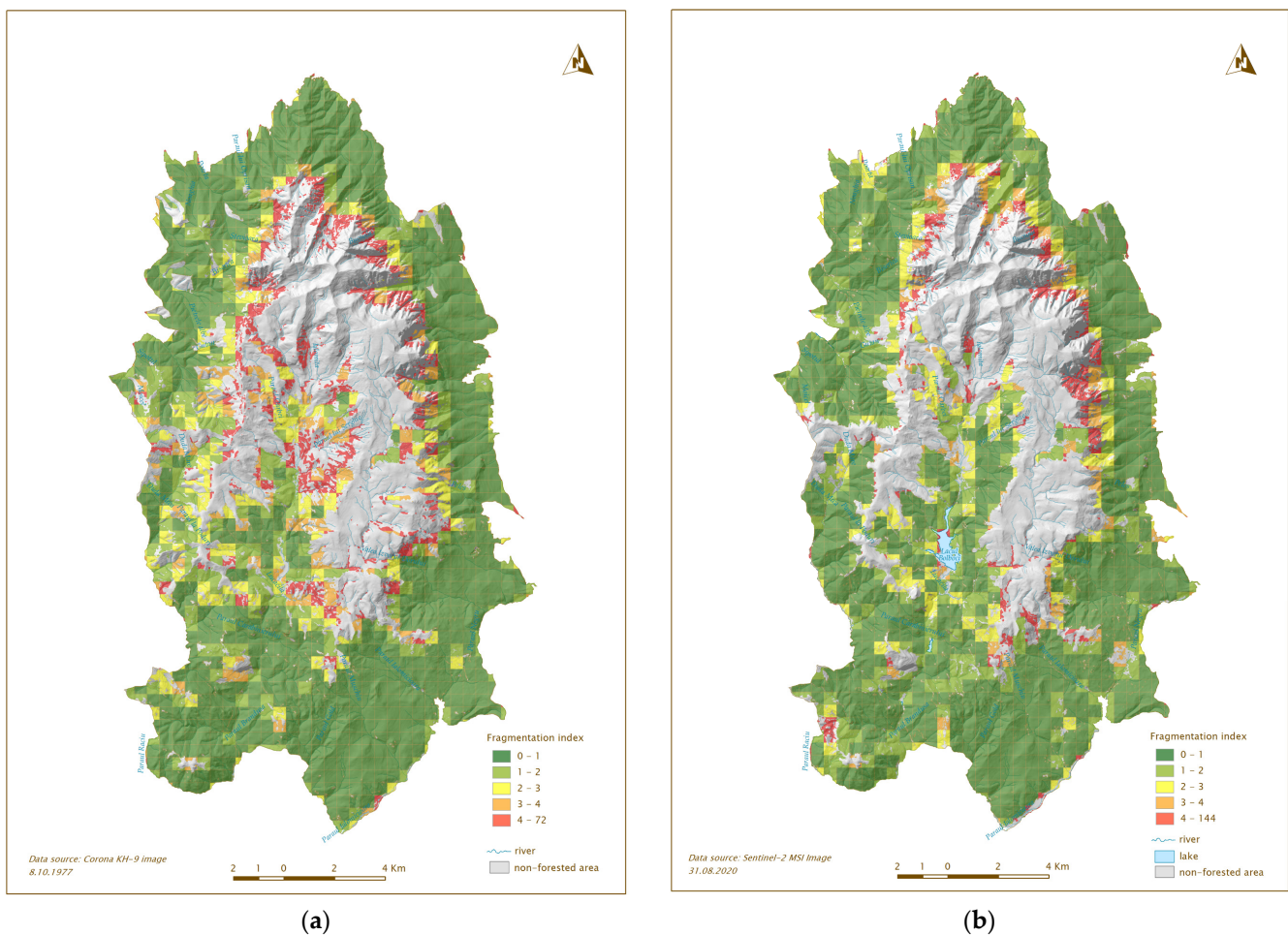


Figure 6. Bucegi Natural Park forest habitat fragmentation maps: (a) 1977 derived from KH-9 orthoimagery; (b) 2020 derived from Sentinel 2-MSI imagery.

The map of the recent situation (2020) (Figure 6b) is an expression of the forest recovery process, as the fragmentation index (density of forest stand patches) decreased from higher than four to 0–1 on most slopes and also in areas close to the river floodplain. This is an indicator of the end of logging activities, as the timber transport infrastructure along the valley turned into tourist access roads (partly modernised along the Ialomița River).

The forest habitat fragmentation maps show that steep slopes still remain a natural fragmentation factor, while the forest recovery process on selected stands features an extended area along the Upper Ialomița Valley. The habitat fragmentation values are higher above 1300 m.

There can also be observed an increase in compacted areas in the forest habitat. The main difference can be seen along the Ialomița Valley, where high values of fragmentation from 1977, flagged with red on the map, were replaced with low values in 2017, marked with green. This situation can also be observed further south, near the Dichiu area or Deleanu and the Tătaru mountains, where the values have improved. There are, however, some areas where the situation has gotten worse, such as the Raciú Mountain in the southwest part of the park near a strictly protected zone, or south of the Dichiu area, where the values went from green to red.

4. Discussion

4.1. Accuracy Assessment of the Images Classifications

The forest landscape in the study area is a key dynamic feature illustrating recent management directions and could be considered a mirror of the protection measures of

the last two decades, especially after the year 2000 when the natural park administration started its activity.

The validation process of both classifications, based on 200 random ground truth points, resulted in a total accuracy assessment of the forest cover class of 99% for the 1977 KH-9 image and 88.5% for the 2020 MSI image (Table 3).

Table 3. Results of validation for the two forest classifications data.

Image Forest Classification	Total Accuracy	Kappa Coefficient
KH-9 hexagon	99%	0.977
Sentinel-2 MSI	88.5%	0.7

The variation in the accuracy values for the two moments can be explained by the difference between the applied methodologies for the image classifications. Thus, for the Corona KH-9 image, segmentation analysis was used, as it is more appropriate for the panchromatic image, resulting in an accuracy of 99%. In this respect, a separation was conducted, and a two-step classification was performed and combined for the final forest habitat layer production. This operation was necessary in order to eliminate the confusion between some shadowed pastures (darker grey) and beech forest-covered areas. The fact highlights the limitations of using panchromatic images in identifying land cover but considering the temporal distance that Corona KH-9 images assure (more than 40 years), this is a small inconvenience to encounter.

For the Sentinel-2 image, a supervised classification method was applied in order to use the multispectral capabilities of the sensor. In this case, a smaller value of 88.5% was obtained due to ground truth points, which were pixels that were randomly placed at the limit of some parcels. This led to some cases where pixel confusion interfered, and although the algorithm had correctly classified the parcel, the truth value went for the nearest category.

4.2. Landscape Metrics in Forest Habitat Fragmentation

Integrating maps with landscape metric-derived data can offer a detailed situation of forest fragmentation. In order to evaluate the accuracy of the approach and to adapt it to the current management issues of the national park, it was necessary to validate the results and evaluate them on characteristic and complementary sites.

Table 4 shows the general trend of forest habitat fragmentation from 1977 to 2020 in the Bucegi Natural Park, Romanian Carpathians, using 10 spatial metrics, starting from the total number of patches and ending with the connectivity variables.

The most representative 10 forested landscape metrics adapted [84,85] to our case studies were selected according to the significance of statistics returned from the forest patch layers modelled from satellite imagery. Their values are also confirmed by the forest and habitat fragmentation maps.

The number of patches index decreased to half of the 1977 parameter, showing that the forest habitat imprint is more compact in 2020 than earlier. It is based on larger patches than before McGarigal, Cushman, Neel and Ene [85] and after the special measures of forest stand reconstruction returned their first results (ex. spruce–fir in Upper Ialomița basin after the 1960s). The strict limitation of timber harvesting after the year 2000, mainly represented by salvage works [86], when the Bucegi Natural Park started to be a reality on the ground, is another possible explanation.

Table 4. Evolution of forest habitat fragmentation in the Bucegi Natural Park, 1977–2020, based on KH-9 imagery and Sentinel 2-MSI classification-derived data.

No.	Class Metrics	Algorithm	UM	Reference Interval	Forest	
					1977	2020
1	Number of patches (NP)	$NP = N$	n/a	$NP > 1$	1493	716
2	Patch density (PD)	$PD = \frac{ni}{A} (10,000)(100)$	nr/100 ha	$PD > 0$	69,848	33,676
3	Landscape shape index (LSI)	$LSI = \frac{0.25 \sum_{k=1}^m eik''}{\sqrt{A}}$	n/a	$LSI \geq 1$	362,246	323,408
4	Connectance index (CONNECT)—1000 M	$CONNECT = \left[\frac{\sum_{j \neq k}^n c_{ijk}}{n_i(n_i-1)} \right] (100)$	%	$0 < CONNECT < 100$	28,102	25,429
5	Euclidian nearest-neighbour index—mean (ENN_{MN})	$ENN_{MN} = \text{mean}(ENN[patch_{ij}])$	m	$ENN_{MN} \geq 0$	404,573	421,778
6	Total area (CA/TA)	$TA = A \left(\frac{1}{10,000} \right)$	ha	$CA \geq 0$	213,750,400	212,614,000
7	Largest patch index (LPI)	$LPI = \frac{\max(a_{ij})}{A} (100)$	%	$0 < LPI < 100$	946,208	979,289
8	Patch area—mean (AREA_MN)	$AREA = a_{ij} \left(\frac{1}{10,000} \right)$	ha	$AREA_{MN} > 0$	143,168	296,947
9	Perimeter-area index—area-weighted mean (PARA_AM)	$AWMSI = \sum_{i=1}^m \sum_{j=1}^n \left[\left(\frac{0.25 p_{ij}}{\sqrt{a_{ij}}} \right) \left(\frac{a_{ij}}{A} \right) \right]$	n/a	$PARA_{AM} > 0$	991,409	887,411
10	Proximity index—area-weighted mean (PROX_AM)	$PROX = \sum_{s=1}^n \frac{a_{ijs}}{h_{ijs}^2}$	m	$PROX_{AM} > 0$	123,309,768	48,952,960

Term explanations. N = total number of patches in the landscape; $i = 1, \dots, m$ or m patch types (classes); $j = 1, \dots, n$ patches; h_{ijs} = distance (m) between patch ijs and patch ijs , based on patch edge-to-edge distance, computed from cell centre to cell centre; a_{ij} = area (m^2) of patch ij ; a_{ijs} = area (m^2) of patch ijs within specified neighbourhood (m) of patch ij ; eik'' = total length (m) of edge in landscape between patch types (classes) i and k ; p_{ij} = perimeter (m) of patch ij ; $ENN[patch_{ij}]$ = the euclidean nearest-neighbour distance of each patch.

The patch density index indicates a similar decreasing trend with the number of patches (a decrease of 50% for the reference period). This means that during the four-decade interval, forest habitats started to be more and more compact towards the timberline or around anthropogenic features such as chalets and roads. There are larger and larger patches, especially after the reforestation of slopes affected by gully erosion was starting to become extinct, mainly on the upper catchment in the Upper Ialomița Valley and its tributaries upstream of the Bolboci reservoir, which was built in 1973. These areas are integrated into the sustainable development area, the lowest level of protection according to the natural park interior zonation.

The landscape shape index of the forest habitats polygon features a slightly decreasing trend, as the patch density is lower and lower, and gullies, ravines on the stream catchments, as well as on former forest roads and paths disappear by grouping around the restoring forest stands (after the spruce–fir patch ages are increasing). The parameter still explains the linear to polygonal grouping of forest stand patches under the superposing natural factors represented by gully and stream erosion (summer season) and avalanches (winter season), together with path and road networks organised between chalets, cable car stations, ski slopes, shepherd huts and communication relays.

The connectance index is almost the same (a slight decrease) and shows a higher degree of discontinuity between the remaining isolated patches along the timberline, where forest stands of spruce–fir pass to the dwarf pine patches on the edges of the high structural plateau to the Ialomița Valley but mainly to the east, where the Prahova Valley is dominated by steep slopes with declivities higher than 40–45 degrees. This is the limited effect of the

topographic and soil cover background at an altitude higher than 1800–1900 m, superposing on the general timberline in the Southern Carpathians.

The Euclidean nearest-neighbouring index mean value for the forest patches illustrates a smooth evolution, as the investigated four decades' general trend was the slight grouping of patches and an increase in the distance between the newer formed groups of forest habitats. This means that smaller, isolated stand patches are more and more integrated into the larger polygons, and the distance between them is increasing, while at the same time, empty spaces between stands (mainly pastures, rock outcrops and eroded surfaces) are becoming smaller or thinner.

The total area index [85] is an expression of continuity in forest habitat coverage between the selected dates, where recovered stands are more and more compact and a timberline patch pattern used to evolve towards a continuous configuration, such as the Upper Ialomița Valley.

The largest patch index is an indicator of the compact coverage of forest habitats within the largest polygon identified for 1977 and 2020. According to the spatial analysis results, this percentage slightly increased from 94 to 97, showing that the compact forest zone belts still feature the outer slopes of the Bucegi Massif as well as the core area of the natural park. This is the result of special management measures around built-up areas to the east, at Sinaia and Bușteni-Poiana Țapului, and continuous forest stand recovery on the Ialomița Valley slopes after the 1950s following systematic projects combined with selective timber harvesting activity in a continuous extinction. After 1973, the main reservoir on the Ialomița River in the mountain area (Bolboci reservoir, 19 million m³) needed a special approach to forest stand conservation and timber harvesting control. This index is another expression of constant forest habitat spatial and temporal development, an encouraging factor for the sustainable development of the protected area.

The patch area statistics index (mean size) is more than double for the 1977–2020 period, showing an important process of forest stand recovery after a period of systematic control of the secondary stands of spruce–fir, fir tree and beech tree. The process was confirmed at the same time by the standard deviation of forest patches, based on the mean size for the reference dates. The 1977 situation featured a bigger fragmentation than the 2020 period, with many patches related to the effects of grazing, the main historical use of the subalpine and alpine zone in the Bucegi Mountains (and still occurs at some points on the structural plateaus and ridges). The timberline was then affected by local clearcutting while some slopes, such as those in the Ialomița Valley, were in the process of forest stand recovery.

The perimeter-area relationship-related index statistics is an expression of the changing pattern of forest habitat for the reference period. The values show a decrease in the perimeter values of the forest habitat corresponding patches. This is an effect of the general trend of smaller patches grouping together with larger ones to the edges of the forest zones, to the timberline, as well as on the stream catchments where recovered stands used to be more and more compact, such as in the Upper Ialomița Valley.

The proximity index shows the degree of patch isolation and fragmentation [87] and is calculated as area-weighted mean values in order to explain the general trend of forest habitat covered patches to join and group with the compact areas towards the integration into the main forest zones. The index shows a significant increase as a result of the isolated forest stands diminution and a clear recovery of the secondary forest stands, although they replaced other primary stands, such as in the Ialomița Valley, where beech stands and beech–spruce–fir stands were replaced by pure spruce–fir stands after the 1950s on highly degraded slopes (Padina, Peștera, Bolboci, Zănoaga areas).

A general view over the pairs of landscape metrics derived from satellite imagery (1977 to 2020) features a general process of forest stand recovery started probably after the closing of large timber harvesting points on the Ialomița Valley and the abandonment of the narrow-gauge railways of the Upper Valley of Ialomița River. This is the case in the Bolboci depressionary area where the timber cable car line to Bușteni, built in 1909 for connecting

the paper factory (established 1882, closed 1990s), was active for more than seven decades until the reservoir of Bolboci formed after building the main dam of the region.

However, there are also areas that have recently been classified with a high level of fragmentation due to massive windthrow that took place in the spring of 2020 (Figure 7). This led to several areas in the park where the trees had to be extracted to leave the forest habitat to recover. Unfortunately, this natural phenomenon, in addition to logging activity from other areas in the park, meant that the fragmentation level in some areas is a dynamic index.

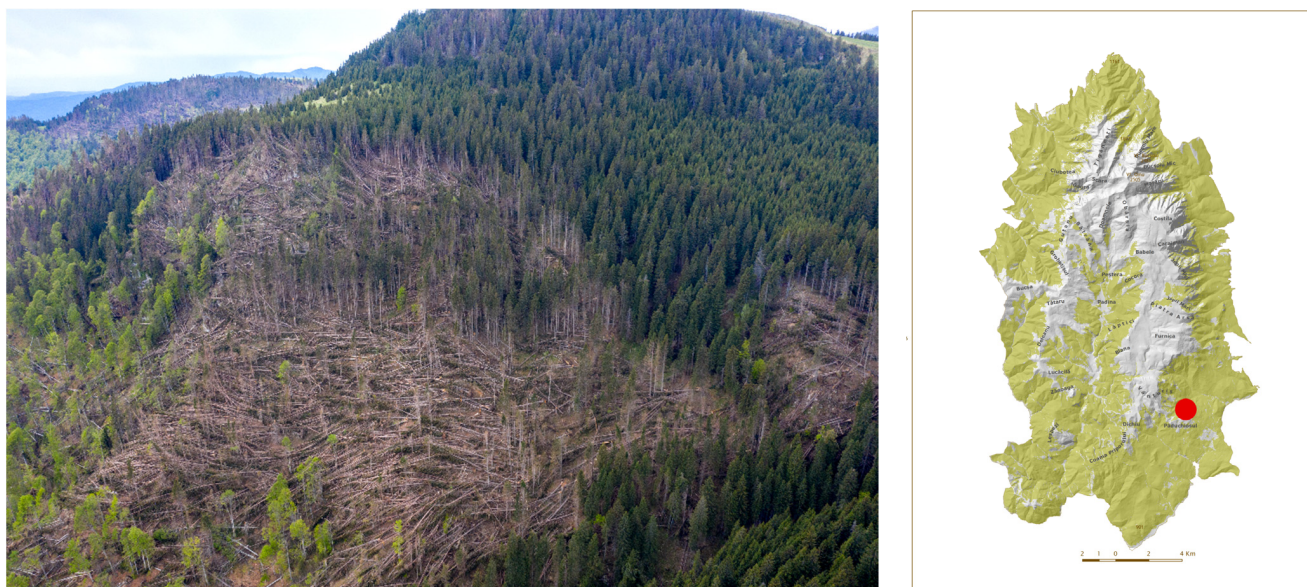


Figure 7. Drone aerial image of forest windthrow—Păduchiosul Mountain, Sustainable Management Zone (Photo: Traian Drăghici, May 2020) The situation map indicates the area the drone image was obtained.

In order to stop activities such as logging or other exploitations, a series of areas with different levels of protection have been designed. In Romania, these are called zones. The Sustainable Development Zone (ZDD on the map—Figure 8) stands for areas where the environment is protected, but there are also permitted a series of economic activities not harmful to the environment. The Sustainable Management Zone (ZMD on the map) protects extensive areas where grazing and logging are permitted as long as the environment is protected and concern is given to the conservation of species. The Integral Protection Zone (ZPI on the map) allows touristic activities and research but without harming or adding any transformation to the environment, while the Strict Protection Zone (ZPS on the map) is meant to protect areas from too many tourists or any damage to the geomorphosites or any vulnerable species that are crossing its limits.

If we are to combine the fragmentation maps with the level of protection map, a series of interesting observations can be made (Figure 8). In this respect, in 1977, one can observe that the ZMD and ZPI areas had high levels of fragmentation, especially in the Upper Ialomița River Basin. Currently, the levels of fragmentation have lowered in many areas, but in some other areas have risen again, such as in the Dichișu area, where new areas have been put under logging exploitation.

The statistics on the level of protection combined with the level of fragmentation of forest habitats (Figure 9) show that high levels have been maintained during the 40-year period in three zones such as the ZMD, ZPI and ZPS. This aspect is to be considered in future measures of permitted activities in the park area. Taking into account the evolution of these parameters, park management can be significantly improved, marking the level of stress factors and the distribution of habitat level of disturbance.

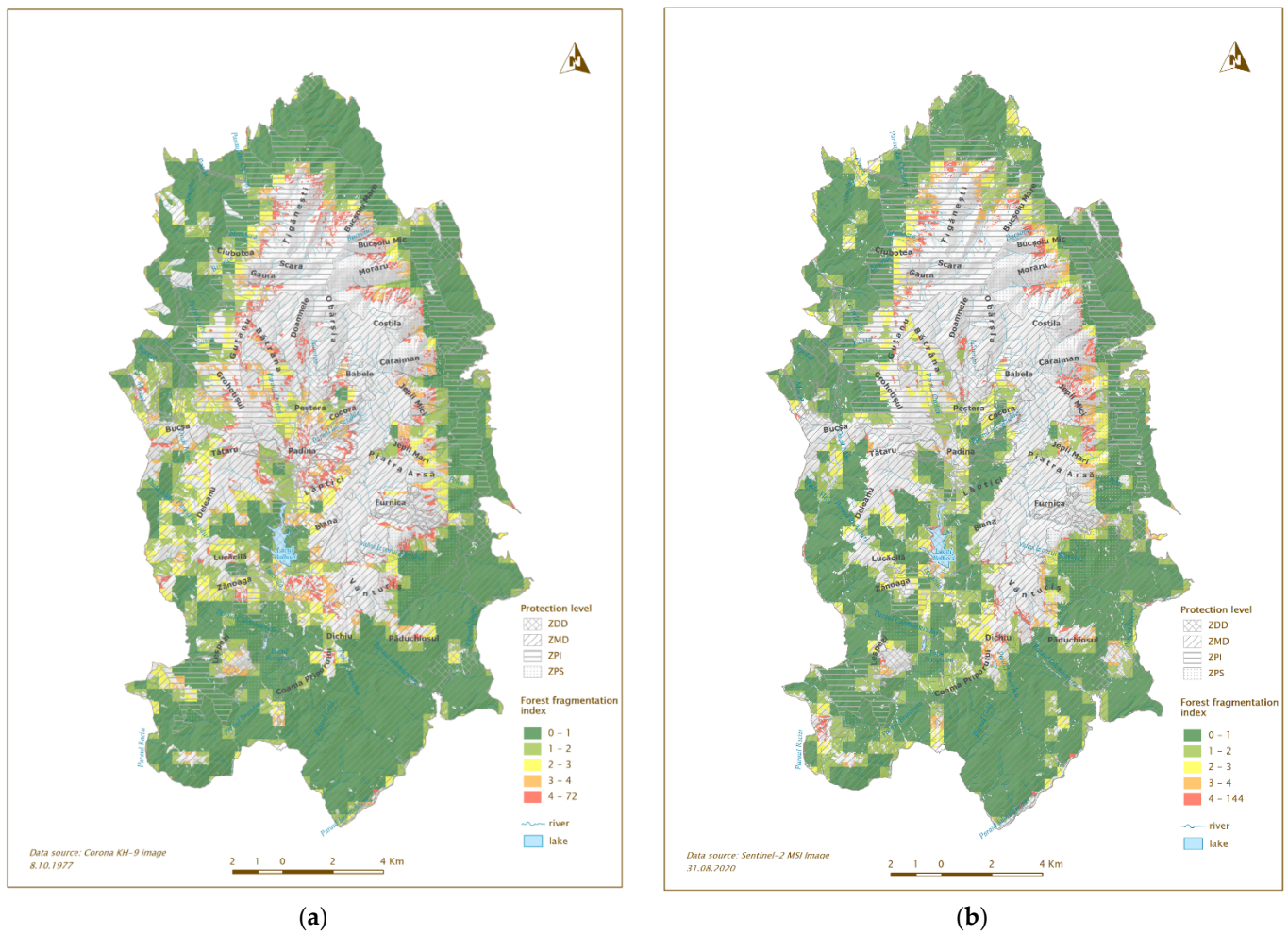


Figure 8. Bucegi Natural Park protection-level maps: ZDD, Sustainable Development Zone; ZMD, Sustainable Management Zone; ZPI, Integral Protection Zone; ZPS, Strict Protection Zone; (a) 1977; (b) 2020.

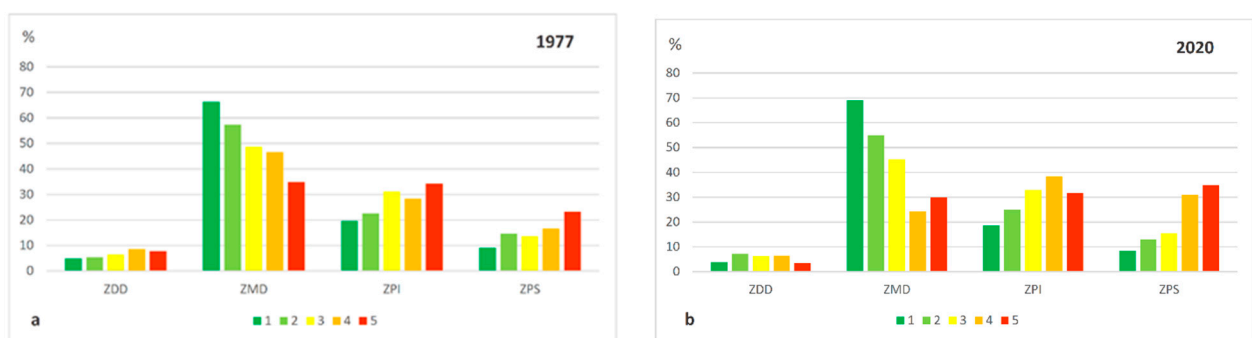


Figure 9. Proportion of fragmentation class per type of protection zone (per cent from class total): ZDD, Sustainable Development Zone; ZMD, Sustainable Management Zone; ZPI, Integral Protection Zone; ZPS, Strict Protection Zone; (a) 1977; (b) 2020.

Considering the management evolution of the natural park in the last 50 years and comparing the maps of the forest habitat, we can conclude that the protection regime must have had a positive effect on the conservation of the forest. Although much of the exploitations observed in the two images overlap, most permissive areas of protection have seen a decrease in fragmentation, a good sign for the habitats and biodiversity.

Even so, the efficiency of the protected areas in the last 30 years is still debatable in Romania since the installation of the democratic regime, and not enough progressive steps have been seen.

Whether evaluating the value for the protected environment [88,89], the level of implication for the local communities and the utilisation of the principles of spatial prioritisation [90], the overall loss of forest stands in protected areas [91] or the lack of use of geospatial tools in order to evaluate and monitor environmental conditions of the protected areas [92], there are still many problems to solve in the context of forest protection and protected area efficacy. In this matter, the use of historical satellite images for environmental studies of protected areas can bring new arguments in establishing rules for protection due to a better understanding of the environment.

4.3. Study Limitations and Future Perspectives

The study emphasised the importance of using historical satellite images in order to obtain evidence of forest evolution and patterns of habitat fragmentation. In this case, however, there are some limitations, as it is very difficult to extract some of the forest species distribution in the classification of historical panchromatic imagery only. This would offer great information on how different species are affected by anthropogenic transformations and why some of them succeed in expanding while others tend to diminish [93].

However, the use of forest cover as the core base of this analysis helped focus on the pattern of evolution and fragmentation of the habitat, which is currently a constant concern [94]. Our study could represent the basis for a prediction analysis, which would evaluate the tendency of forest fragmentation for the next decades, but also the proper measures that are to be taken in order to protect forest cover [95].

Remote sensing data processing in earth observation applications still remains an important tool in the production of basic data layers to be integrated into protected areas mapping and analysis in the context of anthropogenic pressure upon landscapes [96]. Forest habitat fragmentation mapping based on satellite imagery is one of the key directions of this type of approach, usually integrated together with regional biodiversity analysis [45]. Our study also focused on this subject in a close relationship with the international literature [97].

Many recent papers employed Landsat medium-resolution imagery time series, together with selected landscape metrics, to map changes in forest patterns and to evaluate the fragmentation of forest habitats [98–101]. Part of them are dedicated to environmentally protected areas, such as Natura 2000 forested sites [62,102], fragile forest ecosystems under anthropogenic pressure [103,104] or urban-forested grounds [105], but there are other studies with predictive modelling of forest habitats fragmentation [106] based on long-time series analysis.

For the Romanian Carpathian region, a study that focused on the Apuseni Mountains Natural Park [65] employed Landsat time series for three protected areas with complementary regimes and focused on land cover classes corresponding to the main habitat types and not only to forest cover (seven landscape metrics were employed in change detection analysis between 1986 to 2015). Recently, Munteanu et al. (2021) focused on the entire Romanian Carpathian region with a change analysis of forest habitat general coverage between 1955 (Corona imagery) and 2019 (Landsat data mosaics), computing several adapted indices to evaluate the anthropogenic pressure upon high conservation-value forests.

The position of the current approach is new, as this is the first contribution to the Romanian Carpathians using detailed scale modelling of forest cover fragmentation in a protected area. The integration of historical imagery of Corona KH-9 from 1977 was performed using a special photogrammetric approach adapted to the complex topographic context of the Bucegi Natural Park, where the relief index is about 1800 m on a limited surface. This needed an adaptation of the resampling stages in order to produce a high-accuracy orthoimage layer for the classification of forest habitats. Different authors have integrated extended image mosaics of Corona imagery in their studies but have not ex-

plained in detail the geometric accuracies obtained for different features of the terrain on different elevations [55,80].

Newer EO Copernicus data from Sentinel-2 MSI sensors are found as a promising solution in forest cover mapping in forest inventory updates [107] and in biodiversity modelling approaches [97]. In our context, the recent satellite data coverage was used for mapping the entire forest cover of the natural park in order to obtain a compatible layer with the older dataset. The OBIA approach was used by Gil et al. (2013) [50] on multispectral data from IKONOS high-resolution data with four spectral channels plus panchromatic, and Hernando et al. (2017) [51] integrated very high spatial resolution Geo Eye imagery in forest fragmentation mapping and modelling. In our study, the 1977 Corona KH-9 image classification was adapted with a semiautomatic approach of a limited spectral resolution greyscale panchromatic dataset at only 8 bits radiometric resolution. This explains the limitation in the production of a single class forest coverage, without differences between forest types, such as deciduous and coniferous, including dwarf pine canopies, although the recent dataset employed allows spectral classification of these features at a high level of accuracy [67].

Forest fragmentation maps, together with the derived index and the landscape metrics, are the result of GIS analysis at a higher resolution than many other similar contributions focusing on protected areas. They are showing in a synthetic formula the state of the forest cover before and after protected area management started on the ground (2000). Although general statistics can explain a general positive forest canopies recovery, it is interesting to focus on the central part of the region, the Upper Ialomița River Basin. The comparison of maps and the transformation index can explain the role of the timber harvesting points closing after the area was served by a narrow-gauge railway along the main river (built 1905), together with a timber transport line (1906) to the paper factory in Bușteni, which was established in 1882 on Upper Prahova Valley to the east. Although the (secondary) forest stands that recovered after the 1950s are more and more compact, it is also interesting to observe there are effects from windthrows on some slopes with spruce–fir stands, needing more efficiency in management on shallow soils and rock outcrops.

The study has potential practical significance in managing natural park forest cover. Starting from current developments, the spatial database of the Bucegi Natural Park is a work in progress [108]. This was a complex task, as the analysts needed to build a unified forest stand patches layer with their attributes for six forest management units or inspectorates surrounding the Bucegi Massif. They used mainly digitised paper maps from different dates at a 1/20.000 scale, updated every 10 years by field survey and aerial panchromatic image interpretation, integrated to a geodatabase and partly updated with orthophotos at 0.5 m (natural colours and colour infrared images, ANCP Bucharest).

In this respect, the results of our study can provide an accurate forest cover layer for two dates, helping improve understanding of general forest recovery and/or disturbance using a more objective formula. For detailed measurements, the resolution of 10 m is a limiting factor. This can be a problem on steeper slopes where older data layer accuracy needs more attention in forest patch polygon estimation.

5. Conclusions

The analysis of forest habitat fragmentation in the Bucegi Natural Park is an example of integrating two types of remote sensing data from very different sensors in a unitary approach. This is the first study focusing on the forest fragmentation issue in the Romanian Carpathians. The approach comes at a time when, in Romania, there is a lot of debate about forest exploitation and the extension of protected areas as opposite actions upon the environment. In order to compare the Corona KH-9 from 1977 and Sentinel-2 MSI from 2020, we orthorectified image production for the Corona KH-9 at a required accuracy to coregister with the Sentinel-2 MSI image. Building aerial triangulation for the historical dataset was the core of the photogrammetric approach, while the orthorectified product resampling employed derived data from topographic maps. In this context, the single-

channel panchromatic image tested for accuracy was the subject of an integrated visual interpretation and object-based classification approach. In this respect, terrain expertise, together with GIS analysis of the results based on topographic differences, allowed the production of a unitary forest habitat map for 1977.

The resulted fragmentation maps, together with a series of landscape metrics, managed to find a general trend of forest patch dynamics, showing an increase in the level of compactness in several areas of the natural park in the last 40 years.

The foundation of the Bucegi Natural Park has significantly contributed to the level of protection of the area, enabling the forest to extend and recover areas that once have been deforested. The use of historical satellite images in comparison with the ones from today, together with instruments for geospatial analysis of the forest habitats, can significantly improve the management and monitoring of protected areas. Future research should consider the implementation of these instruments and their correlation with other data referring to forest species. This could reveal important changes that occurred in the last decades, raising new questions about the future evolution of the area and the secondary effects on biodiversity.

Author Contributions: Conceptualisation, B.O. and I.S.; methodology, B.O., M.V. and L.T.; software, B.O., M.V. and L.T.; validation, B.O., B.-A.M.; formal analysis, I.S. and M.-G.S.; investigation, B.-A.M. and B.O.; resources, M.V.; data curation, M.-G.S.; writing—original draft preparation, B.-A.M., B.O., M.V., L.T., I.S. and M.-G.S.; writing—review and editing, B.O., I.S., B.-A.M. and M.V.; visualisation, M.-G.S.; supervision, B.O.; project administration, B.O. and M.-G.S.; funding acquisition, I.S. All the authors have equally contributed to this manuscript. All authors have read and agreed to the published version of the manuscript.

Funding: The research has enjoyed the support of the Lifewatch Romania Project (SMIS 126867), financed by the European Union.

Data Availability Statement: Satellite data are publicly available online: Sentinel-2 images were acquired from the Copernicus Open Access Hub (<https://scihub.copernicus.eu> accessed on 15 May 2021). The KH-9 Hexagon images were acquired from the United States Geological Survey (<https://earthexplorer.usgs.gov/> accessed on 25 August 2019). Topographic maps at a scale of 1:25,000 were provided to the Faculty of Geography, University of Bucharest, by the Agenția de Informații Geospațiale a Apărării General de divizie “Constantin Barozzi” (Defense Geospatial Intelligence Agency division General “Constantin Barozzi”).

Acknowledgments: The authors express their gratitude to the editors and anonymous reviewers who contributed to the improvement of the article through their experience, work and comments.

Conflicts of Interest: The authors declare no conflict of interest.

References

1. Kerr, J.T.; Ostrovsky, M. From space to species: Ecological applications for remote sensing. *Trends Ecol. Evol.* **2003**, *18*, 299–305. [[CrossRef](#)]
2. Linke, J.; Betts, M.; Lavrigne, M.; Franklin, S. Structure, Function and Change of Forest Landscapes. In *Understanding Forest Disturbance and Spatial Pattern. Remote Sensing and GIS Approaches*; Wulder, M., Franklin, S., Eds.; CRC Press: Boca Raton, FL, USA, 2006; pp. 1–29.
3. Rose, R.; Byler, D.; Eastman, J.; Fleishman, E.; Geller, G.; Goetz, S.; Guild, L.; Hamilton, H.; Hansen, M.; Headley, R.; et al. Ten Ways Remote Sensing Can Contribute to Conservation. *Conserv. Biol.* **2014**, *29*, 350–359. [[CrossRef](#)]
4. Long, J.A.; Nelson, T.A.; Wulder, M.A. Characterizing forest fragmentation: Distinguishing change in composition from configuration. *Appl. Geogr.* **2010**, *30*, 426–435. [[CrossRef](#)]
5. Innes, J.L.; Koch, B. Forest Biodiversity and Its Assessment by Remote Sensing. *Glob. Ecol. Biogeogr. Lett.* **1998**, *7*, 397–419. [[CrossRef](#)]
6. Healey, S.P.; Cohen, W.B.; Yang, Z.; Kenneth Brewer, C.; Brooks, E.B.; Gorelick, N.; Hernandez, A.J.; Huang, C.; Joseph Hughes, M.; Kennedy, R.E.; et al. Mapping forest change using stacked generalization: An ensemble approach. *Remote Sens. Environ.* **2018**, *204*, 717–728. [[CrossRef](#)]
7. Newton, A.C.; Hill, R.A.; Echeverría, C.; Golicher, D.; Rey Benayas, J.M.; Cayuela, L.; Hinsley, S.A. Remote sensing and the future of landscape ecology. *Prog. Phys. Geogr. Earth Environ.* **2009**, *33*, 528–546. [[CrossRef](#)]

8. Rogan, J.; Miller, J. Integrating GIS and Remotely Sensed Data for Mapping Forest Disturbance and Change. In *Understanding Forest Disturbance and Spatial Pattern. Remote Sensing and GIS Approaches*; Wulder, M., Franklin, S., Eds.; CRC Press: Boca Raton, FL, USA, 2006; pp. 133–172.
9. Ghosh, A.; Munshi, M.; Areendran, G.; Joshi, P.K. Pattern Space Analysis of Landscape Metrics for Detecting Changes in Forests of Himalayan Foothills. *Asian J. GeolInform.* **2012**, *12*.
10. Heilman, G.E.; Strittholt, J.R.; Slosser, N.C.; Dellasala, D.A. Forest Fragmentation of the Conterminous United States: Assessing Forest Intactness through Road Density and Spatial Characteristics: Forest fragmentation can be measured and monitored in a powerful new way by combining remote sensing, geographic information systems, and analytical software. *BioScience* **2002**, *52*, 411–422. [[CrossRef](#)]
11. Wulder, M.A.; White, J.C.; Cranny, M.; Hall, R.J.; Luther, J.E.; Beaudoin, A.; Goodenough, D.G.; Dechka, J.A. Monitoring Canada's forests. Part 1: Completion of the EOSD land cover project. *Can. J. Remote Sens.* **2008**, *34*, 549–562. [[CrossRef](#)]
12. Singh, J.S.; Roy, P.S.; Murthy, M.S.R.; Jha, C.S. Application of landscape ecology and remote sensing for assessment, monitoring and conservation of biodiversity. *J. Indian Soc. Remote Sens.* **2010**, *38*, 365–385. [[CrossRef](#)]
13. Reddy, C.S.; Sreelekshmi, S.; Jha, C.S.; Dadhwal, V.K. National assessment of forest fragmentation in India: Landscape indices as measures of the effects of fragmentation and forest cover change. *Ecol. Eng.* **2013**, *60*, 453–464. [[CrossRef](#)]
14. Turner, W.; Spector, S.; Gardiner, N.; Fladeland, M.; Sterling, E.; Steininger, M. Remote sensing for biodiversity science and conservation. *Trends Ecol. Evol.* **2003**, *18*, 306–314. [[CrossRef](#)]
15. Duro, D.C.; Coops, N.C.; Wulder, M.A.; Han, T. Development of a large area biodiversity monitoring system driven by remote sensing. *Prog. Phys. Geogr. Earth Environ.* **2007**, *31*, 235–260. [[CrossRef](#)]
16. Strand, H.; Hoft, R.; Strittholt, J.; Horning, N.; Miles, L.; Fosnight, E.; Turner, W. (Eds.) *Sourcebook on Remote Sensing and Biodiversity Indicators*; CBD Technical Series No. 32; Secretariat of the Convention on Biological Diversity, NASA-NGO Biodiversity Working Group and the World Conservation Monitoring Centre of the United Nations Environment: Montreal, QC, Canada, 2007.
17. Pettorelli, N.; Wegmann, M.; Skidmore, A.; Mùcher, S.; Dawson, T.P.; Fernandez, M.; Lucas, R.; Schaeppman, M.E.; Wang, T.; O'Connor, B.; et al. Framing the concept of satellite remote sensing essential biodiversity variables: Challenges and future directions. *Remote Sens. Ecol. Conserv.* **2016**, *2*, 122–131. [[CrossRef](#)]
18. Wulder, M.A.; Franklin, S.E. *Understanding Forest Disturbance and Spatial Pattern: Remote Sensing and GIS Approaches*, 1st ed.; CRC Press: Boca Raton, FL, USA, 2006.
19. Paganini, M.; Leidner, A.K.; Geller, G.; Turner, W.; Wegmann, M. The role of space agencies in remotely sensed essential biodiversity variables. *Remote Sens. Ecol. Conserv.* **2016**, *2*, 132–140. [[CrossRef](#)]
20. Garcia, C.A.; Feintrenie, L. Beyond the Mirror: Tropical Forest Fragmentation and Its Impact on Rural Livelihoods. In *Global Forest Fragmentation*; CABI: Wallingford, UK, 2014; pp. 115–131. [[CrossRef](#)]
21. Coops, N.C.; Wulder, M.A.; White, J.C. Identifying and Describing Forest Disturbance and Spatial Pattern: Data Selection Issues and Methodological Implications. In *Understanding Forest Disturbance and Spatial Pattern. Remote Sensing and GIS Approaches*; Wulder, M., Franklin, S., Eds.; CRC Press: Boca Raton, FL, USA, 2006; pp. 31–62.
22. Gillanders, S.N.; Coops, N.C.; Wulder, M.A.; Gergel, S.E.; Nelson, T. Multitemporal remote sensing of landscape dynamics and pattern change: Describing natural and anthropogenic trends. *Prog. Phys. Geogr. Earth Environ.* **2008**, *32*, 503–528. [[CrossRef](#)]
23. Geller, G.N.; Halpin, P.N.; Helmuth, B.; Hestir, E.L.; Skidmore, A.; Ambrams, M.; Aguirre, N.; Blair, M.; Botha, E.; Colloff, M.; et al. Remote Sensing for Biodiversity. In *The GEO Handbook on Biodiversity Observation Networks*; Walters, M., Scholes, R., Eds.; Springer: Cham, Switzerland, 2017.
24. Skole, D.; Tucker, C. Tropical Deforestation and Habitat Fragmentation in the Amazon: Satellite Data from 1978 to 1988. *Science* **1993**, *260*, 1905–1910. [[CrossRef](#)]
25. Wickham, J.D.; O'Neill, R.V.; Jones, K.B. Forest fragmentation as an economic indicator. *Landsc. Ecol.* **2000**, *15*, 171–179. [[CrossRef](#)]
26. Vogelmann, J.E. Assessment of Forest Fragmentation in Southern New England Using Remote Sensing and Geographic Information Systems Technology. *Conserv. Biol.* **1995**, *9*, 439–449. [[CrossRef](#)]
27. Wulder, M. Optical remote-sensing techniques for the assessment of forest inventory and biophysical parameters. *Prog. Phys. Geogr.* **1998**, *22*, 449–476. [[CrossRef](#)]
28. Frohn, R.C. *Remote Sensing for Landscape Ecology: New Metric Indicators for Monitoring, Modeling, and Assessment of Ecosystems*, 1st ed.; CRC Press: Boca Raton, FL, USA, 1997.
29. Jorge, L.A.B.; Garcia, G.J. A study of habitat fragmentation in Southeastern Brazil using remote sensing and geographic information systems (GIS). *For. Ecol. Manag.* **1997**, *98*, 35–47. [[CrossRef](#)]
30. Saura, S. Effects of remote sensor spatial resolution and data aggregation on selected fragmentation indices. *Landsc. Ecol.* **2004**, *19*, 197–209. [[CrossRef](#)]
31. Langford, W.; Gergel, S.; Dietterich, T.; Cohen, W. Map Misclassification Can Cause Large Errors in Landscape Pattern Indices: Examples from Habitat Fragmentation. *Ecosystems* **2006**, *9*, 474–488. [[CrossRef](#)]
32. Gergel, S.E. New directions in landscape pattern analysis and linkages with remote sensing. In *Understanding Forest Disturbance and Spatial Pattern. Remote Sensing and GIS Approaches*; Wulder, M., Franklin, S., Eds.; CRC Press: Boca Raton, FL, USA, 2006; pp. 173–208.
33. Coops, N.C.; Gillanders, S.N.; Wulder, M.A.; Gergel, S.E.; Nelson, T.; Goodwin, N.R. Assessing changes in forest fragmentation following infestation using time series Landsat imagery. *Forest Ecol. Manag.* **2010**, *259*, 2355–2365. [[CrossRef](#)]

34. Jha, C.S.; Goparaju, L.; Tripathi, A.; Gharai, B.; Raghubanshi, A.S.; Singh, J.S. Forest fragmentation and its impact on species diversity: An analysis using remote sensing and GIS. *Biodivers. Conserv.* **2005**, *14*, 1681–1698. [[CrossRef](#)]
35. Roy, P.; Roy, A.; Kushwaha, S.; Singh, S.; Karnatak, H.; Saran, S.; Kushwaha, D.; Porwal, M.C.; Padalia, H.; Nandy, S.; et al. Forest fragmentation in India. *Curr. Sci.* **2013**, *105*, 774–780.
36. Tapia-Armijos, M.F.; Homeier, J.; Espinosa, C.I.; Leuschner, C.; de la Cruz, M. Deforestation and Forest Fragmentation in South Ecuador since the 1970s—Losing a Hotspot of Biodiversity. *PLoS ONE* **2015**, *10*, e0133701. [[CrossRef](#)]
37. Batistella, M.; Robeson, S.; Moran, E. Settlement Design, Forest Fragmentation, and Landscape Change in Rondônia, Amazônia. *Photogramm. Eng. Remote Sens.* **2003**, *69*, 805–812. [[CrossRef](#)]
38. Carranza, M.L.; Frate, L.; Acosta, A.T.R.; Hoyos, L.; Ricotta, C.; Cabido, M. Measuring forest fragmentation using multitemporal remotely sensed data: Three decades of change in the dry Chaco. *Eur. J. Remote Sens.* **2014**, *47*, 793–804. [[CrossRef](#)]
39. Ramachandra, T.V.; Setturu, B.; Chandran, S. Geospatial analysis of forest fragmentation in Uttara Kannada District, India. *For. Ecosyst.* **2016**, *3*, 10. [[CrossRef](#)]
40. Gong, C.; Yu, S.; Joesting, H.; Chen, J. Determining socioeconomic drivers of urban forest fragmentation with historical remote sensing images. *Landsc. Urban Plan* **2013**, *117*, 57–65. [[CrossRef](#)]
41. Zhou, W.; Zhang, S.; Yu, W.; Wang, J.; Wang, W. Effects of Urban Expansion on Forest Loss and Fragmentation in Six Megaregions, China. *Remote Sens.* **2017**, *9*, 991. [[CrossRef](#)]
42. Bryan-Brown, D.N.; Connolly, R.M.; Richards, D.R.; Adame, F.; Friess, D.A.; Brown, C.J. Global trends in mangrove forest fragmentation. *Sci. Rep.* **2020**, *10*, 7117. [[CrossRef](#)] [[PubMed](#)]
43. Hermosilla, T.; Wulder, M.A.; White, J.C.; Coops, N.C.; Pickell, P.D.; Bolton, D.K. Impact of time on interpretations of forest fragmentation: Three-decades of fragmentation dynamics over Canada. *Remote Sens. Environ.* **2019**, *222*, 65–77. [[CrossRef](#)]
44. Armenteras, D.; González, T.M.; Retana, J. Forest fragmentation and edge influence on fire occurrence and intensity under different management types in Amazon forests. *Biol. Conserv.* **2013**, *159*, 73–79. [[CrossRef](#)]
45. Reddy, C.S.; Kurian, A.; Srivastava, G.; Singhal, J.; Varghese, A.O.; Padalia, H.; Ayyappan, N.; Rajashekar, G.; Jha, C.S.; Rao, P.V.N. Remote sensing enabled essential biodiversity variables for biodiversity assessment and monitoring: Technological advancement and potentials. *Biodivers. Conserv.* **2021**, *30*, 1–14. [[CrossRef](#)]
46. Sahana, M.; Sajjad, H.; Ahmed, R. Assessing spatio-temporal health of forest cover using forest canopy density model and forest fragmentation approach in Sundarban reserve forest, India. *Model. Earth Syst. Environ.* **2015**, *1*, 49. [[CrossRef](#)]
47. Lawley, V.; Lewis, M.; Clarke, K.; Ostendorf, B. Site-based and remote sensing methods for monitoring indicators of vegetation condition: An Australian review. *Ecol. Indic.* **2016**, *60*, 1273–1283. [[CrossRef](#)]
48. Renó, V.; Novo, E.; Escada, M. Forest Fragmentation in the Lower Amazon Floodplain: Implications for Biodiversity and Ecosystem Service Provision to Riverine Populations. *Remote Sens.* **2016**, *8*, 886. [[CrossRef](#)]
49. Harper, G.; Steininger, M.; Tucker, C.; Juhn, D.; Hawkins, F. Fifty Years of Deforestation and Forest Fragmentation in Madagascar. *Environ. Conserv.* **2007**, *34*, 325–333. [[CrossRef](#)]
50. Gil, A.; Lobo, A.; Abadi, M.; Silva, L.; Calado, H. Mapping invasive woody plants in Azores Protected Areas by using very high-resolution multispectral imagery. *Eur. J. Remote Sens.* **2013**, *46*, 289–304. [[CrossRef](#)]
51. Hernando, A.; Velázquez, J.; Valbuena, R.; Legrand, M.; García-Abril, A. Influence of the resolution of forest cover maps in evaluating fragmentation and connectivity to assess habitat conservation status. *Ecol. Indic.* **2017**, *79*, 295–302. [[CrossRef](#)]
52. Taubert, F.; Fischer, R.; Groeneveld, J.; Lehmann, S.; Müller, M.S.; Rödig, E.; Wiegand, T.; Huth, A. Global patterns of tropical forest fragmentation. *Nature* **2018**, *554*, 519–522. [[CrossRef](#)] [[PubMed](#)]
53. Tappan, G.; Hadj, A.; Wood, E.; Lietzow, R.W. Use of Argon, Corona, and Landsat Imagery to Assess 30 Years of Land Resource Changes in West-Central Senegal. *Photogramm. Eng. Remote Sens.* **2000**, *66*, 727–735.
54. Quanjun, J.; Bing, Z.; Liangyun, L. The feasibility of landscape pattern analysis within the alpine steppe of the Yellow River source based on historical CORONA panchromatic imagery. *Proc. SPIE* **2012**, *8538*, 85381N.
55. Rendenieks, Z.; Nita, M.D.; Nikodemus, O.; Radeloff, V.C. Half a century of forest cover change along the Latvian-Russian border captured by object-based image analysis of Corona and Landsat TM/OLI data. *Remote Sens. Environ.* **2020**, *249*, 112010. [[CrossRef](#)]
56. Munteanu, C.; Senf, C.; Nita, M.D.; Sabatini, F.M.; Oeser, J.; Seidl, R.; Kuemmerle, T. Using historical spy satellite photographs and recent remote sensing data to identify high-conservation-value forests. *Conserv. Biol.* **2021**, *36*, e13820. [[CrossRef](#)]
57. Mihai, A.B.; Nedelcu, A.; Buterez, C.; Cruceru, I.; Olariu, B.; Rujoiu-Mare, M.R.; Savulescu, I.; Tudose, I. *Județul Prahova. Spațiu, Societate, Economie, Mediu*; Editura Academiei Române: Bucharest, Romania, 2016.
58. Nistor, C.; Virghileanu, M.; Carlan, I.; Mihai, B.-A.; Toma, L.; Olariu, B. Remote Sensing-Based Analysis of Urban Landscape Change in the City of Bucharest, Romania. *Remote Sens.* **2021**, *13*, 2323. [[CrossRef](#)]
59. Klimetzek, D.; Stăncioiu, P.T.; Paraschiv, M.; Niță, M.D. Ecological Monitoring with Spy Satellite Images—The Case of Red Wood Ants in Romania. *Remote Sens.* **2021**, *13*, 520. [[CrossRef](#)]
60. Nagendra, H.; Lucas, R.; Honrado, J.P.; Jongman, R.H.G.; Tarantino, C.; Adamo, M.; Mairota, P. Remote sensing for conservation monitoring: Assessing protected areas, habitat extent, habitat condition, species diversity, and threats. *Ecol. Indic.* **2013**, *33*, 45–59. [[CrossRef](#)]
61. Soverel, N.O.; Coops, N.C.; White, J.C.; Wulder, M.A. Characterizing the forest fragmentation of Canada’s national parks. *Environ. Monit. Assess.* **2010**, *164*, 481–499. [[CrossRef](#)] [[PubMed](#)]

62. Gounaridis, D.; Zaimis, G.; Koukoulas, S. Quantifying spatio-temporal patterns of forest fragmentation in Hymettus Mountain, Greece. *Comput. Environ. Urban Syst.* **2014**, *46*, 35–44. [[CrossRef](#)]
63. Giriraj, A.; Murthy, M.S.; Beierkuhnlein, C. Evaluating forest fragmentation and its tree community composition in the tropical rain forest of Southern Western Ghats (India) from 1973 to 2004. *Environ. Monit. Assess.* **2010**, *161*, 29–44. [[CrossRef](#)] [[PubMed](#)]
64. Sharma, K.; Robeson, S.; Thapa, P.; Saikia, A. Land-use/land-cover change and forest fragmentation in the Jigme Dorji National Park, Bhutan. *Phys. Geogr.* **2016**, *38*, 1–18. [[CrossRef](#)]
65. Chețan, M.A.; Dornik, A.; Urdea, P. Analysis of recent changes in natural habitat types in the Apuseni Mountains (Romania), using multi-temporal Landsat satellite imagery (1986–2015). *Appl. Geogr.* **2018**, *97*, 161–175. [[CrossRef](#)]
66. Huzui, A.; Abdelkader, A.; Patru-Stupariu, I. Analysing urban dynamics using multi-temporal satellite images in the case of a mountain area, Sinaia (Romania). *Int. J. Digit. Earth* **2013**, *6*, 563–579. [[CrossRef](#)]
67. Rujoiu-Mare, M.-R.; Olariu, B.; Mihai, B.-A.; Nistor, C.; Săvulescu, I. Land cover classification in Romanian Carpathians and Subcarpathians using multi-date Sentinel-2 remote sensing imagery. *Eur. J. Remote Sens.* **2017**, *50*, 496–508. [[CrossRef](#)]
68. Toader, T.; Dumitru, I. *Pădurile României—Parcuri Naționale și Parcuri Naturale*; Regia Națională a Pădurilor: Bucharest, Romania, 2004.
69. PNB. *Parcul Natural Bucegi—Plan de Management*; Regia Națională a Pădurilor—Romsliva: Bucharest, Romania, 2018.
70. NRO. *HEXAGON American's Eyes in Space Fact Sheet*; National Reconnaissance Office, Center for the Study of National Reconnaissance: Chantilly, VA, USA, 2011.
71. Galiatsatos, N.; Donoghue, D.N.; Philip, G. High resolution elevation data derived from stereoscopic CORONA imagery with minimal ground control. *Photogramm. Eng. Remote Sens.* **2007**, *73*, 1093–1106. [[CrossRef](#)]
72. Surazakov, A.; Aizen, V. Positional accuracy evaluation of declassified Hexagon KH-9 mapping camera imagery. *Photogramm. Eng. Remote Sens.* **2010**, *76*, 603–608. [[CrossRef](#)]
73. Drusch, M.; Del Bello, U.; Carlier, S.; Colin, O.; Fernandez, V.; Gascon, F.; Hoersch, B.; Isola, C.; Laberinti, P.; Martimort, P.; et al. Sentinel-2: ESA's Optical High-Resolution Mission for GMES Operational Services. *Remote Sens. Environ.* **2012**, *120*, 25–36. [[CrossRef](#)]
74. ESA. *Sentinel-2 User Handbook*; European Space Agency (ESA): Paris, France, 2015.
75. Fletcher, K. *Sentinel-2: ESA's Optical High-Resolution Mission for GMES Operational Services*; ESA Communications: Noordwijk, The Netherlands, 2012.
76. USGS. *Declassified Intelligence Satellite Photographs Summary of Satellite Missions*; USGS: Reston, VA, USA, 2008.
77. Burnett, M.G. *Hexagon (KH-9) Mapping Program and Evolution*; Center for the Study of National Reconnaissance: Chantilly, VA, USA, 1982.
78. McGlone, J.C.; Mikhail, E.M.; Bethel, J.S.; Mullen, R. *Manual of Photogrammetry*, 5th ed.; American Society for Photogrammetry and Remote Sensing: Baton Rouge, LA, USA, 2004.
79. ASPRS. New Asprs Positional Accuracy Standards for Digital Geospatial Data Released. *Photogramm. Eng. Remote Sens.* **2015**, *81*, 277. [[CrossRef](#)]
80. Nita, M.D.; Munteanu, C.; Gutman, G.; Abrudan, I.V.; Radeloff, V.C. Widespread forest cutting in the aftermath of World War II captured by broad-scale historical Corona spy satellite photography. *Remote Sens. Environ.* **2018**, *204*, 322–332. [[CrossRef](#)]
81. Lusier, J.D.; Thompson, W.L.; Wilson, J.M.; Gorham, B.E.; Dragut, L.D. Using digital photographs and object-based image analysis to estimate percent ground cover in vegetation plots. *Front. Ecol. Environ.* **2006**, *4*, 408–413. [[CrossRef](#)]
82. Lewis, H.G.; Brown, M. A generalized confusion matrix for assessing area estimates from remotely sensed data. *Int. J. Remote Sens.* **2001**, *22*, 3223–3235. [[CrossRef](#)]
83. Gómez, C.; White, J.C.; Wulder, M.A. Optical remotely sensed time series data for land cover classification: A review. *ISPRS J. Photogramm. Remote Sens.* **2016**, *116*, 55–72. [[CrossRef](#)]
84. McGarigal, K.; Marks, B.J. FRAGSTATS. Spatial pattern analysis program for quantifying landscape structure. Version 2.0. In *Forest Science Department*; Oregon State University: Corvallis, OH, USA, 1994; p. 67.
85. McGarigal, K.S.; Cushman, S.; Neel, M.; Ene, E. *FRAGSTATS: Spatial Pattern Analysis Program for Categorical Maps*; Landscape Ecology Lab, University of Massachusetts: Amherst, MA, USA, 2002.
86. Yang, Z.; Kennedy, R.; Cohen, W.; Healey, S. Remotely Sensed Data in the Mapping of Forest Harvest Patterns. In *Understanding Forest Disturbance and Spatial Pattern*; CRC Press: Boca Raton, FL, USA, 2006; pp. 63–84.
87. Affek, A.; Degórski, M.; Wolski, J.; Solon, J.; Kowalska, A.; Roo-Zielińska, E.; Grabińska, B.; Kruczkowska, B. Chapter 3—Methods. In *Ecosystem Service Potentials and Their Indicators in Postglacial Landscapes*; Affek, A., Degórski, M., Wolski, J., Solon, J., Kowalska, A., Roo-Zielińska, E., Grabińska, B., Kruczkowska, B., Eds.; Elsevier: Amsterdam, The Netherlands, 2020; pp. 97–111.
88. Comănescu, L.; Nedelea, A. Public perception of the hazards affecting geomorphological heritage—Case study: The central area of Bucegi Mts. (Southern Carpathians, Romania). *Environ. Earth Sci.* **2015**, *73*, 8487–8497. [[CrossRef](#)]
89. Cucu, L.A.; Niculae, M.-I.; Pătroescu, M. Hierarchical analysis of the threats for Species of Community Interest in the Iron Gates Natural Park, Romania. *Forum Geogr.* **2013**, *XII*, 52–58. [[CrossRef](#)]
90. Ioja, C.I.; Patroescu, M.; Rozyłowicz, L.; Popescu, V.D.; Verghelet, M.; Zotta, M.L.; Felciuc, M. The efficacy of Romania's protected areas network in conserving biodiversity. *Biol. Conserv.* **2010**, *143*, 2468–2476. [[CrossRef](#)]

91. Knorn, J.A.N.; Kuemmerle, T.; Radeloff, V.C.; Keeton, W.S.; Gancz, V.; Biriş, I.-A.; Svoboda, M.; Griffiths, P.; Hagatis, A.; Hostert, P. Continued loss of temperate old-growth forests in the Romanian Carpathians despite an increasing protected area network. *Environ. Conserv.* **2012**, *40*, 182–193. [[CrossRef](#)]
92. Olariu, B. Metode de analiză a calității mediilor montane în arile protejate. In *Studiu de Caz: Parcul Natural Bucegi*; University of Bucharest: Bucharest, Romania, 2019.
93. Huebner, C.D.; Randolph, J.C.; Parker, G.R. Environmental Factors Affecting Understory Diversity in Second-Growth Deciduous Forests. *Am. Midl. Nat.* **1995**, *134*, 155–165. [[CrossRef](#)]
94. Fischer, R.; Taubert, F.; Müller Michael, S.; Groeneveld, J.; Lehmann, S.; Wiegand, T.; Huth, A. Accelerated forest fragmentation leads to critical increase in tropical forest edge area. *Sci. Adv.* **2021**, *7*, eabg7012. [[CrossRef](#)] [[PubMed](#)]
95. Batar, A.K.; Shibata, H.; Watanabe, T. A Novel Approach for Forest Fragmentation Susceptibility Mapping and Assessment: A Case Study from the Indian Himalayan Region. *Remote Sens.* **2021**, *13*, 4090. [[CrossRef](#)]
96. Nagendra, H.; Mairota, P.; Marangi, C.; Lucas, R.; Dimopoulos, P.; Honrado, J.P.; Niphadkar, M.; Múcher, C.A.; Tomaselli, V.; Panitsa, M.; et al. Satellite Earth observation data to identify anthropogenic pressures in selected protected areas. *Int. J. Appl. Earth Obs. Geoinf.* **2015**, *37*, 124–132. [[CrossRef](#)]
97. Cavender-Bares, J.; Schneider, F.D.; Santos, M.J.; Armstrong, A.; Carnaval, A.; Dahlin, K.M.; Fatoyinbo, L.; Hurtt, G.C.; Schimel, D.; Townsend, P.A.; et al. Integrating remote sensing with ecology and evolution to advance biodiversity conservation. *Nat. Ecol. Evol.* **2022**, *6*, 506–519. [[CrossRef](#)] [[PubMed](#)]
98. Muhammed, A.; Elias, E. Class and landscape level habitat fragmentation analysis in the Bale mountains national park, southeastern Ethiopia. *Heliyon* **2021**, *7*, e07642. [[CrossRef](#)]
99. Narmada, K.; Dhanusree, G.D.; Bhaskaran, G. Landscape metrics to analyze the forest fragmentation of Chitteri Hills in Eastern Ghats, Tamil Nadu. *J. Civ. Eng. Environ. Sci.* **2021**, *7*, 001–007. [[CrossRef](#)]
100. Pyngrope, O.R.; Kumar, M.; Pebam, R.; Singh, S.K.; Kundu, A.; Lal, D. Investigating forest fragmentation through earth observation datasets and metric analysis in the tropical rainforest area. *SN Appl. Sci.* **2021**, *3*, 705. [[CrossRef](#)]
101. Halbgewachs, M.; Wegmann, M.; da Ponte, E. A Spectral Mixture Analysis and Landscape Metrics Based Framework for Monitoring Spatiotemporal Forest Cover Changes: A Case Study in Mato Grosso, Brazil. *Remote Sens.* **2022**, *14*, 1907. [[CrossRef](#)]
102. Mengist, W.; Soromessa, T.; Feyisa, G.L. Forest fragmentation in a forest Biosphere Reserve: Implications for the sustainability of natural habitats and forest management policy in Ethiopia. *Resour. Environ. Sustain.* **2022**, *8*, 100058. [[CrossRef](#)]
103. Da Silva, A.L.; de Nunes, A.J.N.; Marques, M.L.; Ribeiro, A.Í.; Longo, R.M. Assessing the fragility of forest remnants by using landscape metrics. Comparison between river basins in Brazil and Portugal. *Environ. Monit. Assess.* **2021**, *193*, 172. [[CrossRef](#)]
104. Solano, F.; Praticò, S.; Piovesan, G.; Chiarucci, A.; Argentieri, A.; Modica, G. Characterizing historical transformation trajectories of the forest landscape in Rome’s metropolitan area (Italy) for effective planning of sustainability goals. *Land Degrad. Dev.* **2021**, *32*, 4708–4726. [[CrossRef](#)]
105. Kowe, P.; Mutanga, O.; Dube, T. Advancements in the remote sensing of landscape pattern of urban green spaces and vegetation fragmentation. *Int. J. Remote Sens.* **2021**, *42*, 3797–3832. [[CrossRef](#)]
106. De Keersmaecker, W.; Rodríguez-Sánchez, P.; Milencović, M.; Herold, M.; Reiche, J.; Verbesselt, J. Evaluating recovery metrics derived from optical time series over tropical forest ecosystems. *Remote Sens. Environ.* **2022**, *274*, 112991. [[CrossRef](#)]
107. Coops, N.C.; Tompalski, P.; Goodbody, T.R.H.; Achim, A.; Mulverhill, C. Framework for near real-time forest inventory using multi source remote sensing data. *For. Int. J. For. Res.* **2022**, cpac015. [[CrossRef](#)]
108. Badea, O. *Cercetări Ecologice pe Termen Lung în Ecosisteme Forestiere Reprezentative din Parcul Natural Bucegi*; Badea, O., Ed.; Editura Silvică: Voluntari, Romania, 2013.